A Buckboost-Buck PFC rectifier as an LED driver

BISWAJIT PATTANAIK

A Dissertation Submitted to

Indian Institute of Technology Hyderabad

In Partial Fulfillment of the Requirements for

The Degree of Master of Technology

भारतीय प्रौद्योगिकी संस्थान हैदराबाद
Indian Institute of Technology Hyderabad

Department of Electrical Engineering

June, 2015

Declaration

I declare that this written submission represents my ideas in my own words, and where others' ideas or words have been included, I have adequately cited and referenced the original sources. I also declare that I have adhered to all principles of academic honesty and integrity and have not misrepresented or fabricated or falsified any idea/data/fact/source in my submission. I understand that any violation of the above will be a cause for disciplinary action by the Institute and can also evoke penal action from the sources that have thus not been properly cited, or from whom proper permission has not been taken when needed.

Biswajit Pattanaik

(Signature)

BISWAJIT PATTANAIK

(Student Name)

EE12M1009

(Roll No)

Approval Sheet

This thesis entitled A Buckboost-Buck PFC rectifier as an LED driver by Biswajit Pattanaik is approved for the degree of Master of Technology from IIT Hyderabad.

Dr. Pradeep Yemula
Department of Electrical Engineering
Indian Institute of Technology Hyderabad
Examiner

Dr. G Ramesh
Department of Mathematics
Indian Institute of Technology Hyderabad
Examiner

Dr. Siva Kumar K
Department of Electrical Engineering
Indian Institute of Technology Hyderabad
Adviser

Vaskar Sarkar
Dr. Vaskar Sarkar
Department of Electrical Engineering
Indian Institute of Technology Hyderabad
Chairman

Acknowledgements

I would like to express my gratitude towards my supervisor Dr. K. Siva Kumar for giving me a chance to work on such a memorable project and for his exemplary guidance, monitoring and constant encouragement throughout the course of this thesis. The blessing, help and guidance given by him time to time shall carry me a long way in the journey of life on which I am about to embark. I would also like to thank research scholars and masters students of Power Electronics and Power Systems who have helped me either directly or indirectly. I would like to thank all my friends for their support.

Dedicated to

My Parents, My Supervisor & My friends

Abstract

The objective of this thesis is to design a buckboost-buck power factor corrector (PFC) to drive a string of High Brightness Light Emitting Diodes (HB-LEDs). Conventional buck-boost converter is used for power factor correction, but it suffers from issues like the inverted polarity of the output voltage, floating drive requirement for its active switch. These issues have been addressed in the proposed PFC converter by an integration of buck-boost and buck topologies. The PFC converter is able to drive load, with nearly unity power factor, significantly low input current total harmonic distortion (THD) with higher efficiency of power conversion. The theoretical analysis and operation of the proposed converter with an 20W LED load have been verified by simulation in MATLAB/Simulink. Finally, the experimental results of a laboratory prototype with an output power of 20W supplied from 110v/50Hz are provided to validate the simulation results.

Nomenclature

CCM : Continuous conduction mode

PFC : Power factor corrected

DCM : Discontinuous conduction mode

PIV : Peak Inverse Voltage

THD : Total Harmonic Distortion

SMPS: Switched Mode Power Supplies

Irms : R.M.S current

Ipeak: Peak current

HB-LEDs: High Brightness Light Emitting Diodes

f_S: Switching frequency

Contents

Chapter 1

Introduction

1.1 Motivation

These days, high-brightness light-emitting diodes (HB-LEDs) are becoming very attractive options for lighting applications because they possess characteristics such as low power consumption, high efficiency, long lifespan, low maintenance, environmental friendliness (due to absence of mercury), high reliability, high robustness etc [1-2].

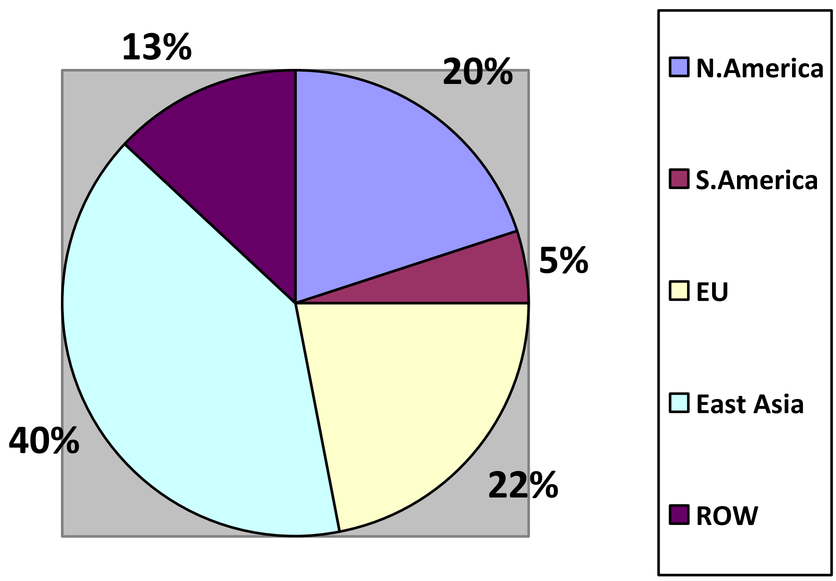

Figure1.1(a)Market Share by Region,2010

Source: Green Market Research

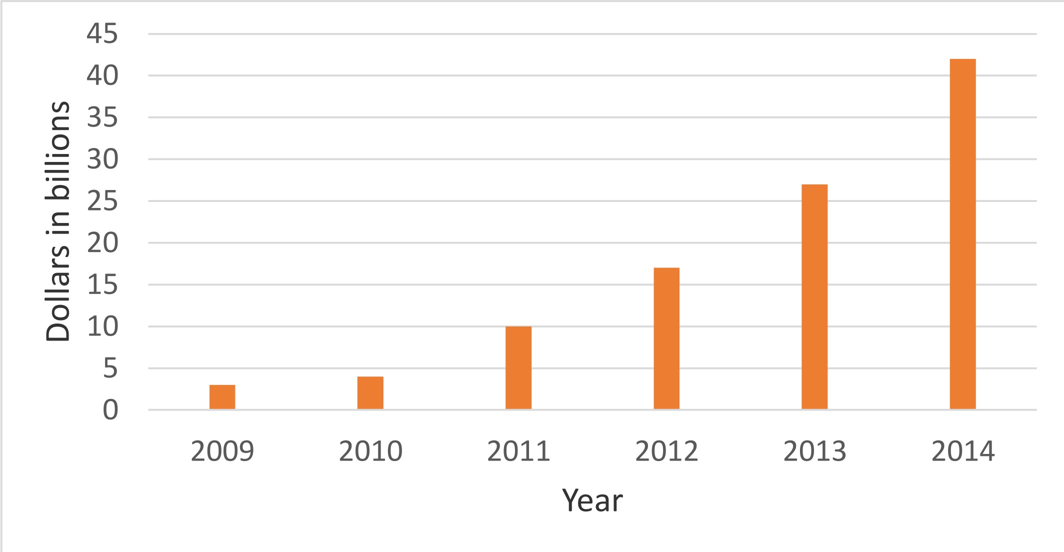

Figure 1.1 (b): Global market for LED lighting

Source: Digitimes

The Figure 1.1(a) shows worldwide market share of LED lighting system as of 2010. As LED lamps generally last around 50,000 hours against 1000 hours for incandescent and 10,000 hours for CFLs, maintenance requirements are less. Further, reduction in CO2 emissions by using LEDs is a major advantage. These advantages led to the wide spread use of HB-LEDs in LCD backlight, automobile industry, traffic light, decorative lighting and general purpose lighting etc. [3-4].

Table 1.1: Comparison of Certain Characteristics of Different Light Sources

	Incandescent[22]	Halogen [23]	CFL [24]	LED(Cree) [25]	LED(LEDNovation) [26]
Purchase Price(dollars)	.41	1.5	.99	9.97	31.50
Power used(watts)	60	43	14	9.5	9.4
Lumens (mean)	860	750	775	800	810
Lumens/watt	14.3	17.4	55.4	84	86.2
Lifespan (hours)	1000	1000	10000	25000	50000
Bulb lifetime inyears@6hours/day	.46	.46	4.6	11.4	22.8
Energy cost over 20 years @13 cents/kWh	$342	$245	$80	$54	$57
Totalcost per 860 lumens 860 lumens	$360	$356	$93	$80	$86

1.2 LED Driver Circuit

The HB-LEDs being diodes are driven by dc supply, but when the supply is an AC source, a conventional bridge rectifier along with modern switched mode power supplies (SMPSs) is ubiquitously used [5-6]. These cause poor power-factor and high total harmonic distortion (THD) owing to their non-linear behavior. High harmonic content deteriorates the power quality and is detrimental to the system performance [7-8]. To improve the power quality, input power factor and input current THD must be within limits of EN 61000-3-2 class C regulations [9]. A power factor corrected (PFC) converter can improve the power-factor as well as lower the THD which can be either of two stages or single stage. Despite several advantages of a two stage PFC converter, it suffers from certain shortcomings like reduced efficiency due to two stage processing of input power, higher cost because of higher number of components and reliability [5]. Hence single stage topologies are preferred which are more efficient.

1.3 System Description

In order to improve the power quality for LED lightings, an alternative power factor corrected converter is proposed. The power factor corrected (PFC) Rectifier is a combination of a bridge rectifier and proposed PFC converter. A universal voltage controller IC is used to sense the load voltage and correct it as per system requirement.

1.4 EN61000-3-2 class C regulation (for $P \leq 25$ Watts)

- The third harmonic current, expressed as a percentage of the fundamental current, shall not exceed 86% and the fifth shall not exceed 61%.

- The waveform of the input current shall be such that it begins to flow before or at 60^0, has its last peak peaks per half period(if there are several peaks per half period)) before or at 65^0 and does not stop flowing before 90^0, where the zero crossing of the fundamental supply voltage is assumed to be at 0^0

Chapter 2

Proposed Circuit Analysis, Design & Control

2.1 Proposed Circuit

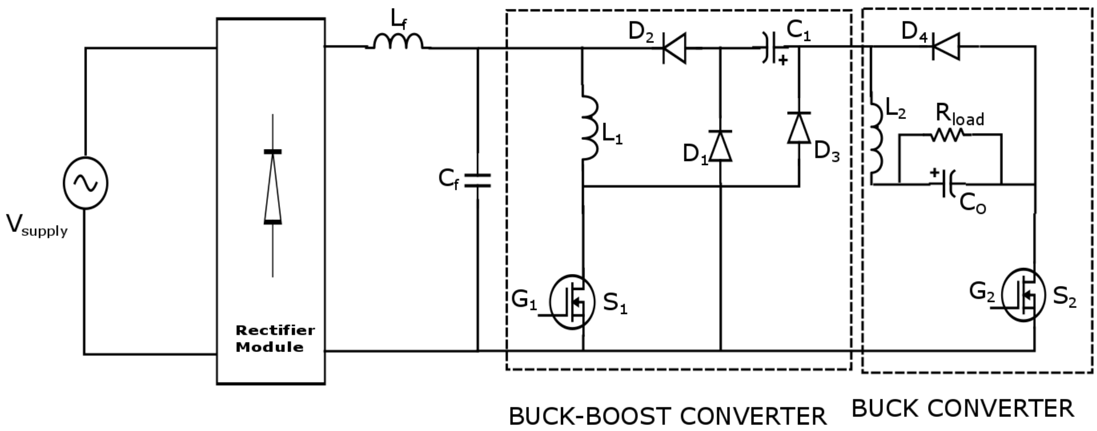

Figure 2.1: Schematic of Proposed PFC Circuit

The circuit diagram of the proposed converter is shown in Figure 2.1. This is a non-inverting, integrated Buckboost-buck converter. The buck-boost converter consists of one inductor$\left(L_1\right)$, one capacitor$\left(C_1\right)$, three diodes$\left(D_1, D_2, D_3\right)$and one controlled switch$\left(S_1\right)$. The buck-boost converter is operated in discontinuous conduction mode (DCM) to improve the input power factor. The output stage buck converter consists of one inductor$\left(L_2\right)$, one controlled switch$\left(S_2\right)$, one diode$\left(D_4\right)$and one capacitor$\left(C_O\right)$for providing a constant output voltage. The mode of operation of the buck converter hardly affects the input power factor, but to achieve several advantages like zero current switching of the controlled switch during turn on and fast regulation of the output voltage, the buck converter is operated in DCM [12]. Buck-Boost converter is generally preferred for power factor correction for it has the highest power factor correction capability when operated in DCM.

2.2 Advantages

The advantages of the proposed integrated PFC converter are as follows:

- Output and input of the PFC converter are of same polarity during turn on;
- Sources of the controlled switches S_1 and S_2 are connected to the same potential hence they can be driven by gate pulses without floating drivers;
- R.m.s current flowing through each controlled switch is reduced at the expense of two separate switches S_1 and S_2 for buck-boost and buck stages respectively reducing current stress across the controlled switches thereby decreasing the conduction loss and increasing the efficiency.

2.3 Analysis of the proposed circuit

To analyze the proposed converter fallowing assumptions are made for better understanding [12]:

- The input supply voltage is a pure sine wave free from all kinds of non-linearity i.e. $|V_S| = |V_m \sin \omega t|$, where V_m is the peak amplitude and ω is the angular frequency of the supply voltage;
- All the components of the PFC converters are taken as ideal which will make the analysis simpler.
- Switching frequency is taken very large compared to the supply frequency, so input voltage can be assumed as almost constant during one switching period T_S;

- L_1 and L_2 values are taken such as both will operate in DCM and L_1 enters DCM before L_2
- To achieve a low ripple at the output voltage, a large capacitor C_O is taken.

The operation of PFC can be described in four different modes as shown in Figure-2.3 over one switching cycle T_S.

Mode-I$\left(0 < t < D_1 T_S\right)$: Prior to this mode, the capacitor C_1 stores energy from the discharge of the input inductor L_1 and becomes fully charged. This mode is described in Figure-2.4(a). Let's assume that at the start of this mode the initial currents through L_1 and L_2 are zero because both the inductors are made to operate in DCM. This mode starts when both the switches S_1 and S_2 are turned ON simultaneously at time t=0. Diodes D_3 and D_4 are reverse biased whereas only diode D_1 is forward biased during this mode. Input inductor L_1 comes directly across the input rectified voltage source $|V_S| = |V_m \sin \omega t|$ and gets charged by the supply voltage itself. The input current $\left(I_{in}\right)$ passes through inductor L_1 and switch S_1 .Inductor current $\left(I_{L_1}\right)$ and S_1 switch current $\left(I_{S_1}\right)$ increase linearly as can be seen in Figure-3. The peak values of the current through the switch, inductor current and supply current are as follows:

$$\left\langle I_{L_1} \right\rangle_{Peak} = \left\langle I_{S_1} \right\rangle_{Peak} = \left\langle I_{in} \right\rangle_{Peak} = \frac{V_m \left|\sin(\theta)\right|}{L_1} D_1 T_S \tag{2.1}$$

During this mode the capacitor discharges and the current freewheels through L_2 , load, S_2 and and D_1 the respective current waveforms can be seen in Figure-2.5.

Mode-II $(D_1T_S < t < D_2T_S)$ **:** This period begins with the removal of gate pulses to both the switches and I_{S_1}, I_{S_2} fall to zero instantaneously causing the switches S_1 and S_2 to be reverse biased. The currents I_{L_1} and I_{L_2} start to decay linearly. I_{L_1} freewheels through L_1, D_3, C_1 and D_2 till it decays to zero at and C_1 gets charged by this discharging current. In a similar fashion, I_{L_2} freewheels through L_2, load and D_4 as can be seen from Figure-2.4(b).The respective current waveforms can be seen in Figure-2.5.

Mode-III $(D_2T_S < t < D_3T_S)$**:** In this mode, the current I_{L_2} continues to decay linearly till it becomes zero at t_2.Figure-2.4(c) illustrates this mode of operation and the current waveforms can be seen from Figure-2.5.

Mode-IV $(D_3T_S < t < T_S)$**:** During this mode, the output bulk capacitor C_O energizes the load. Generally, the capacitor taken is large enough to provide an almost constant output voltage.

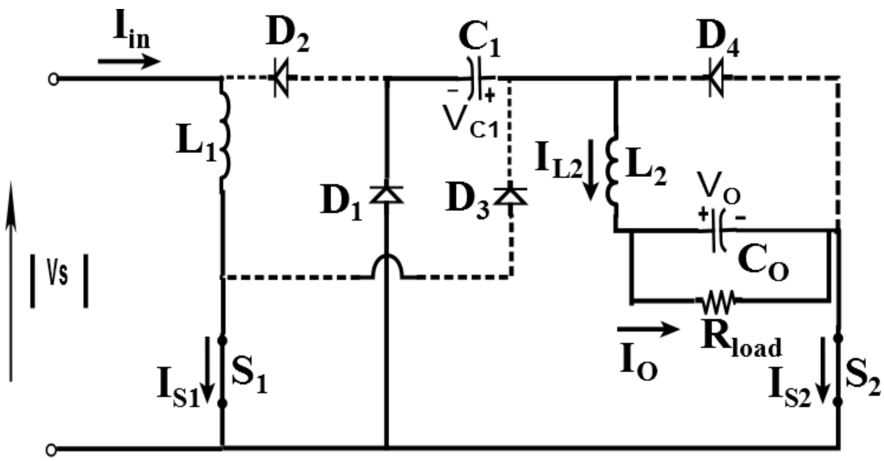

Figure 2.4 (a): Equivalent circuit in Mode-1 operation

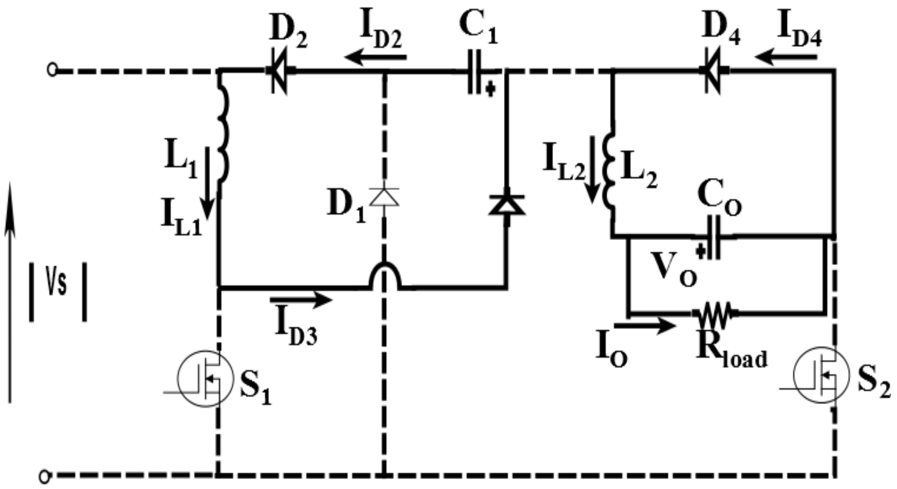

Figure 2.4 (b): Equivalent circuit in Mode-2 operation

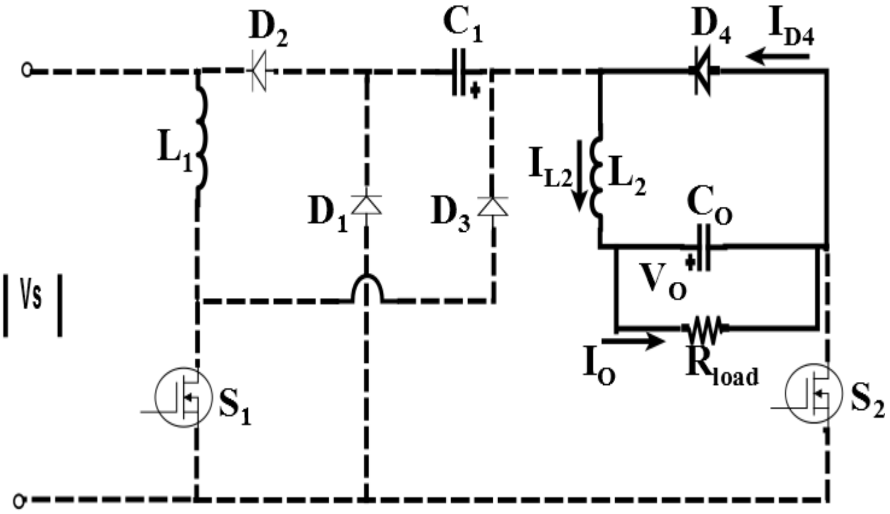

Figure 2.4 (c): Equivalent circuit in Mode-3 operation

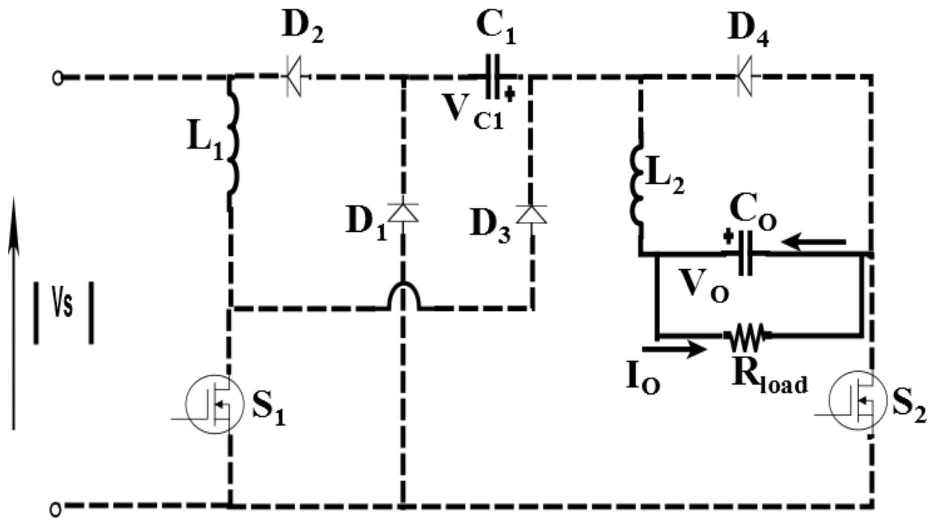

Figure 2.4 (d): Equivalent circuit in Mode-4 operation

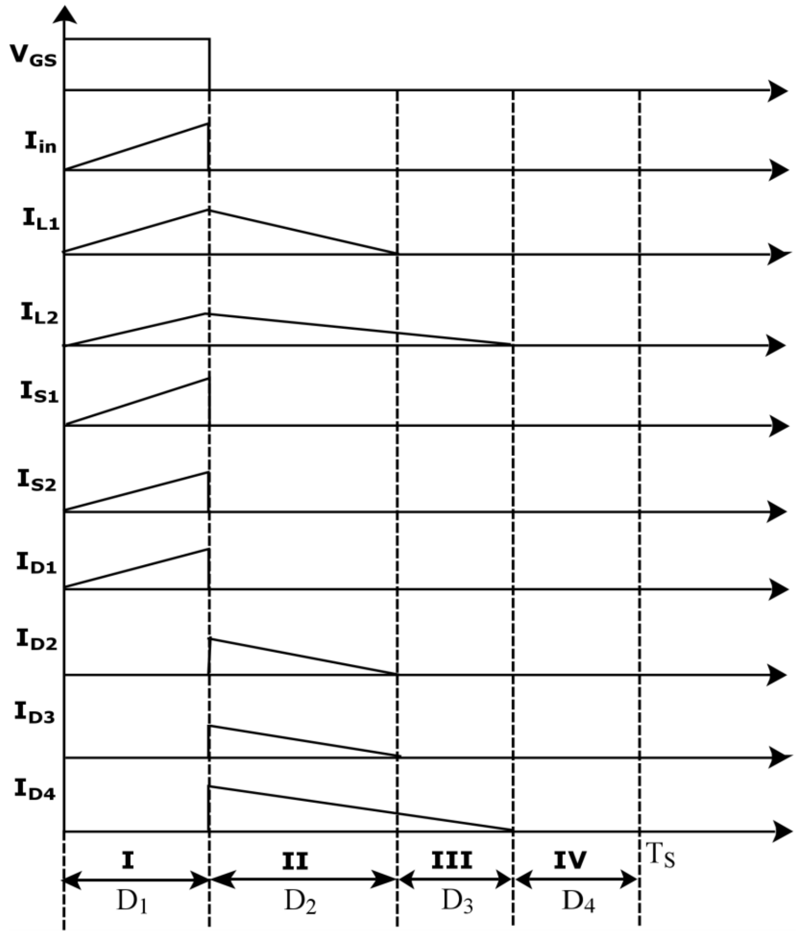

Fig.2.5 Different current waveforms of the proposed PFC converter during one T_S

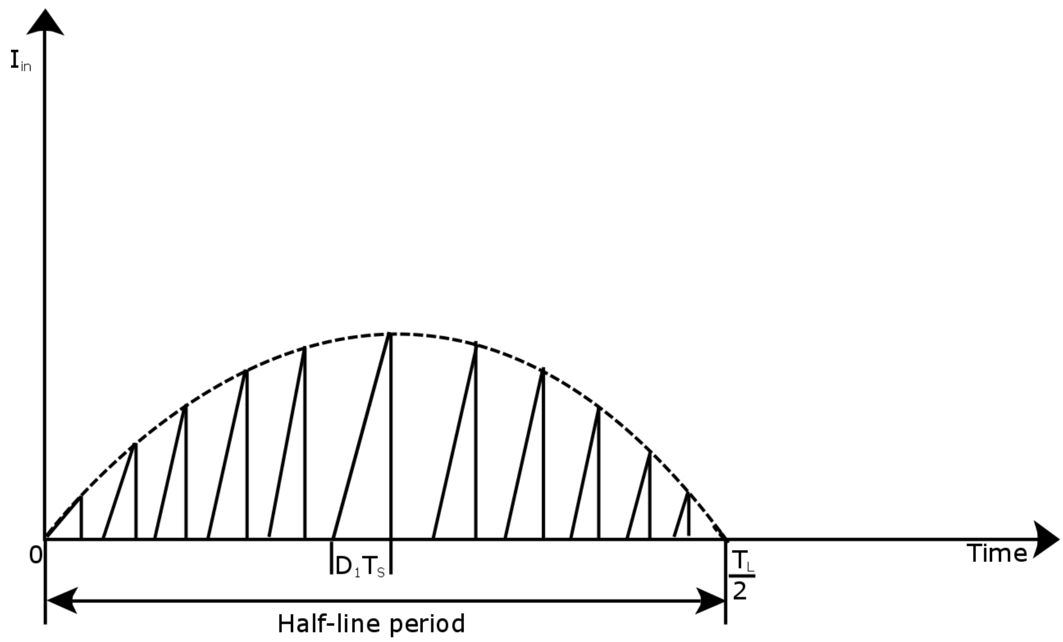

Figure 2.5: Input Current To the PFC During Half-line Period

The input buck-boost converter operates in DCM. The input current is tringular in nature as can be seen in the above Figure 2.5.

$$\left\langle I_{in} \right\rangle_{Peak} = \frac{V_m \sin \omega_l t}{L_1} D_1 T_S \tag{2.2}$$

$$\left\langle I_{in} \right\rangle_{avg} = \frac{1}{2} \times \frac{1}{T_S} \times \left\langle I_{in} \right\rangle_{peak} \times D_1 \times T_S \tag{2.3}$$

$$\left\langle I_{in} \right\rangle_{avg} = \frac{D_1^2 V_m \sin \omega_l t}{2 L_1 f_S} \tag{2.4}$$

Assuming the input voltage and input current to be be in phase, the input power to the converter is

$$\Rightarrow \left\langle P_{in} \right\rangle_{avg} = \frac{1}{2} \times V_m \times I_m$$

$$\Rightarrow \left\langle P_{in} \right\rangle_{avg} = \frac{D_1^2 V_m^2}{4 L_1 f_S} \tag{2.5}$$

Output load power assuming the load voltage is constant

$$\langle P_O \rangle_{avg} = \frac{V_O^2}{R_{load}} \tag{2.6}$$

With an assumption of 100% efficiency[15],

$$P_{in} = P_O$$

$$\Rightarrow \frac{D_1^2 V_m^2}{4 L_1 f_s} = \frac{V_O^2}{R_{load}}$$

$$\Rightarrow V_O = \frac{D_1 V_m}{2\sqrt{\frac{L_1 f_s}{R_{load}}}} \tag{2.7}$$

Equation(2.7) indicates that the output voltage not only depends upon on period (D_1) but also on buck-boost inductor (L_1),switching frequency (f_s) and load (R_{load}). Varying any one of them will result a change in the output voltage. From Equation(2.7), we can also determine the approximate value of D_1 which will be described later in this section. All the analysis done below in this section are similar to the analysis done in[17, 18].

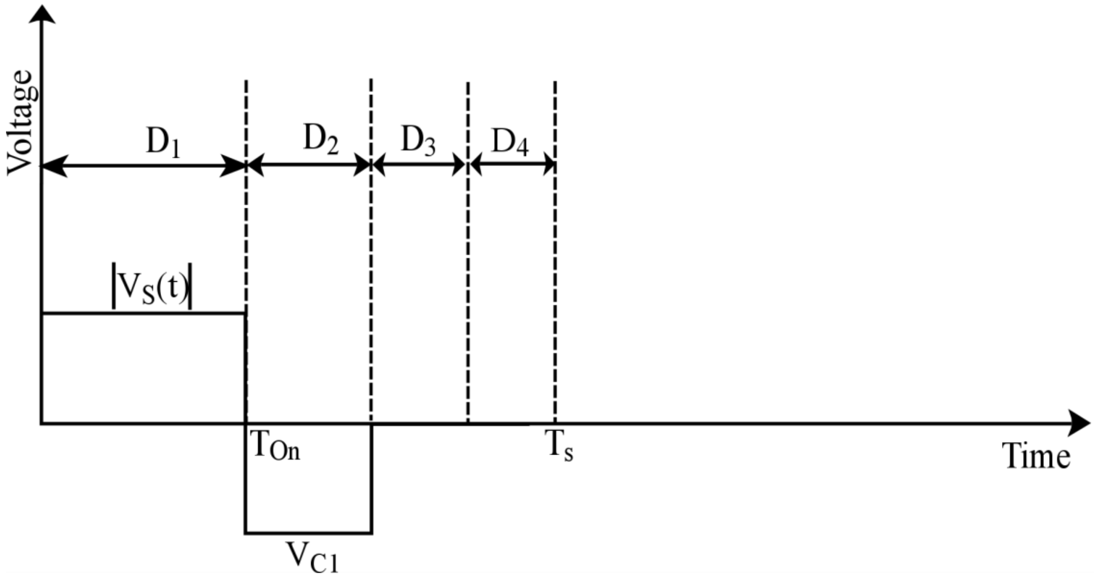

Figure 2.6: Voltage wave form across the buck-boost inductor

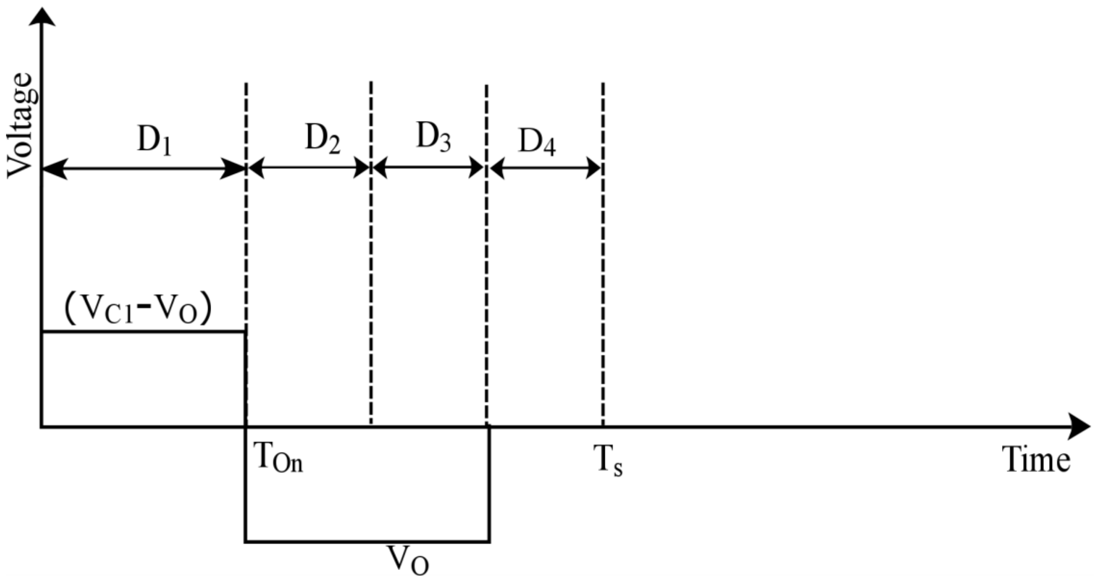

Figure 2.7: Voltage wave form across the buck inductor

Figure 2.6 shows the voltage waveform across the buck-boost inductor (L_1). Applying volt-sec balance across L_1, we will get

$$D_1 \left| V_S(t) \right| = V_{C_1} D_2$$

$$\Rightarrow D_1 \times \left(\frac{|V_S(t)|}{V_{C_1}} \right) = D_2 \qquad (2.8)$$

Figure 2.7 shows the voltage waveform across the buck inductor (L_2). Applying volt-sec balance across L_2, we will get

$$\left(V_{C_1} - V_O\right) D_1 = V_O \left(D_2 + D_3\right)$$

$$\Rightarrow D_2 + D_3 = \left[\frac{V_{C_1} - V_O}{V_O} \right] D_1 \qquad (2.9)$$

Putting the equation (2.8) in equation (2.9), we will get

$$\Rightarrow D_3 = \left[\frac{V_{C_1} - V_O}{V_O} - \frac{|V_S(t)|}{V_{C_1}} \right] D_1 \qquad (2.10)$$

2.3.1 R.m.s current rating of the Switches and Reactive components

Mathematical derivation of r.m.s current rating of the switches and reactive components are done in this section [17, 18]. The results are then compared with the simulation results in next section which will be helpful in selecting devices of proper rating for hardware implementation.

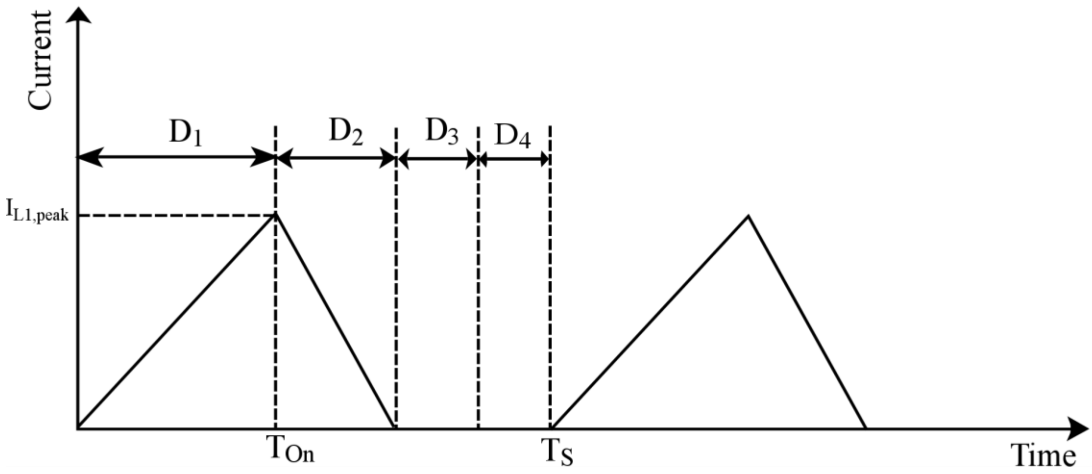

Figure 2.8: Current wave form of the buck-boost inductor

The above figure shows the current flowing in L_1. As the inductor is being operated in DCM, the current waveform is triangular in nature. The current rises till T_{On} before falling to zero at the end of D_2T_s period. The formula for r.m.s current of the switch over the switching period T_s is

$$\left\langle I_{L_1,rms} \right\rangle_{T_S} = I_{L_1,peak}\sqrt{\frac{\left(D_1 + D_2\right)}{3}} \tag{2.11}$$

Using the Equation (2.8) in the current formula above, we will get

$$\Rightarrow \left\langle I_{L_1,rms} \right\rangle_{T_S} = I_{L_1,peak}\sqrt{\frac{D_1}{3}}\sqrt{1+\frac{\left|V_S(\theta)\right|}{V_{C_1}}}$$

$$\Rightarrow \left\langle I_{L_1,rms} \right\rangle_{T_S} = \frac{\left|V_S(\theta)\right|}{f_S L_1}\sqrt{\frac{\left(D_1\right)^3}{3}}\sqrt{1+\frac{\left|V_S(\theta)\right|}{V_{C_1}}} \tag{2.12}$$

Where

$$I_{L_1,peak} = \frac{\left|V_S(\theta)\right|}{f_S L_1} D_1$$

The formula for the r.m.s current over the half-line period $\left(\frac{T_L}{2}\right)$ can be found out by integrating over the half-line period

$$\left\langle I_{L_1,rms} \right\rangle_{\frac{T_L}{2}} = \frac{1}{\pi f_S L_1} \sqrt{\frac{\left(D_1\right)^3}{3} \int_0^{\pi} \left|V_S(\theta)\right| \sqrt{1 + \frac{\left|V_S(\theta)\right|}{V_{C_1}}} d\theta} \tag{2.13}$$

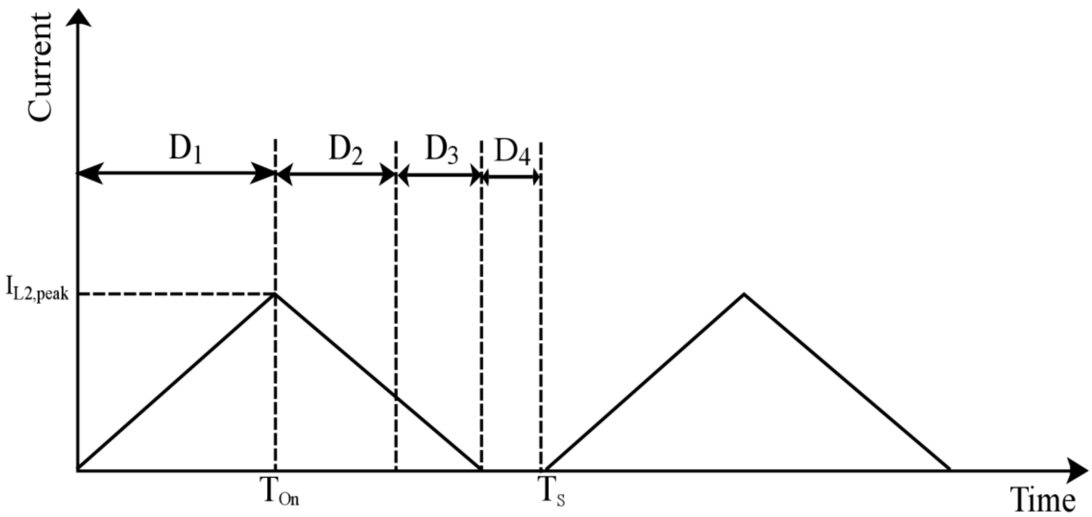

Figure 2.9: Current wave form of the buck inductor

The above figure shows the current flowing in L_2. As the inductor is being operated in DCM, the current waveform is triangular in nature. The current rises till T_{On} before falling to zero at the end of switching period. The formula for r.m.s current of the switch over the switching period T_s can be found out in a similar manner

$$\left\langle I_{L_2,rms} \right\rangle_{T_S} = I_{L_2,peak} \sqrt{\frac{D_1 + D_2 + D_3}{3}} \tag{2.14}$$

Using equations (2.9),(2.10)and(2.14), we will get

$$\Rightarrow \left\langle I_{L_2,rms} \right\rangle_{T_S} = \frac{I_{L_2,peak}}{\sqrt{3}} \sqrt{D_1 + D_1 \frac{\left|V_S(\theta)\right|}{V_{C_1}} + D_1 \left[\frac{V_{C_1} - V_O}{V_O} - \frac{\left|V_S(\theta)\right|}{V_{C_1}} \right]}$$

$$\Rightarrow \left\langle I_{L_2,rms} \right\rangle_{T_S} = \frac{\left(V_{C_1} - V_O\right)}{f_S L_2} \sqrt{\frac{\left(D_1\right)^3}{3}} \sqrt{\left[\frac{V_{C_1}}{V_O}\right]} \tag{2.15}$$

Where

$$I_{L_2,peak} = \frac{\left(V_{C_1} - V_O\right)}{f_S L_2} D_1$$

The formula for the r.m.s current over the half-line period $\left(\frac{T_L}{2}\right)$ can be found out by integrating over the half-line period

$$\left\langle I_{L_2,rms} \right\rangle_{\frac{T_L}{2}} = \frac{\left(V_{C_1} - V_O\right)}{f_S L_2} \sqrt{\frac{\left(D_1\right)^3}{3}} \sqrt{\frac{V_{C_1}}{V_O}} \tag{2.16}$$

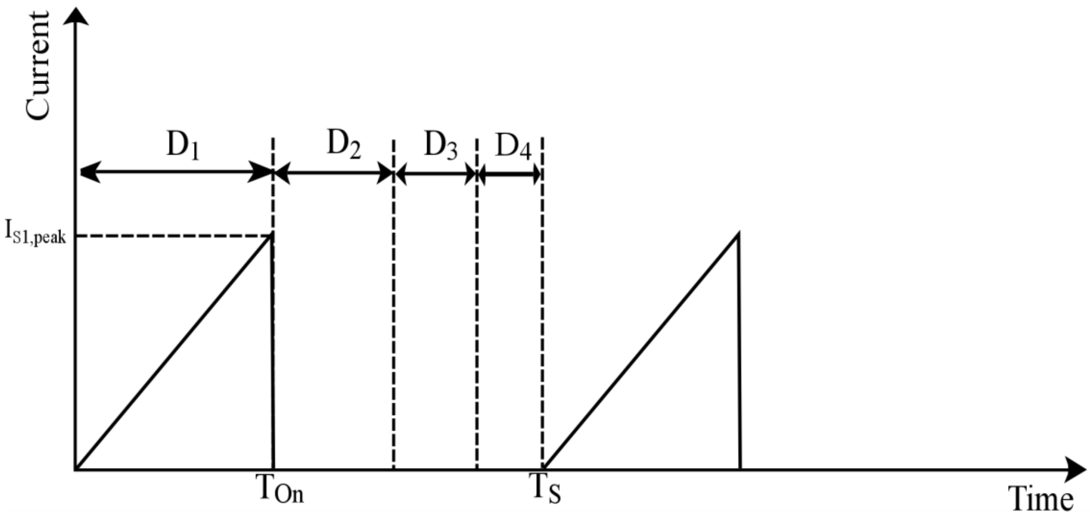

Figure 2.10: Current wave form of the Switch S1

The above figure shows the current flowing through S_1.The current rises till T_{On} before falling to zero at the end of ON period. The current through the switch is identical with the current flowing through the inductor till T_{on}.The formula for r.m.s current of the switch over the switching period T_s can be found out in a similar manner

$$\left\langle I_{S_1,rms} \right\rangle_{T_S} = I_{S_1,peak} \sqrt{\frac{D_1}{3}}$$

$$\Rightarrow \left\langle I_{S_1,rms} \right\rangle_{T_S} = \frac{\left| V_S(\theta) \right|}{f_S L_1} \sqrt{\frac{\left(D_1\right)^3}{3}} \tag{2.17}$$

Where

$$I_{S_1,peak} = \frac{\left| V_S(\theta) \right|}{L_1} D_1 T_S$$

The formula for the r.m.s current over the half-line period $\left(\frac{T_L}{2}\right)$ can be found out by integrating over the half-line period

$$\left\langle I_{S_1,rms} \right\rangle_{\frac{T_L}{2}} = \frac{2V_m}{\pi f_S L_1} \sqrt{\frac{\left(D_1\right)^3}{3}} \tag{2.18}$$

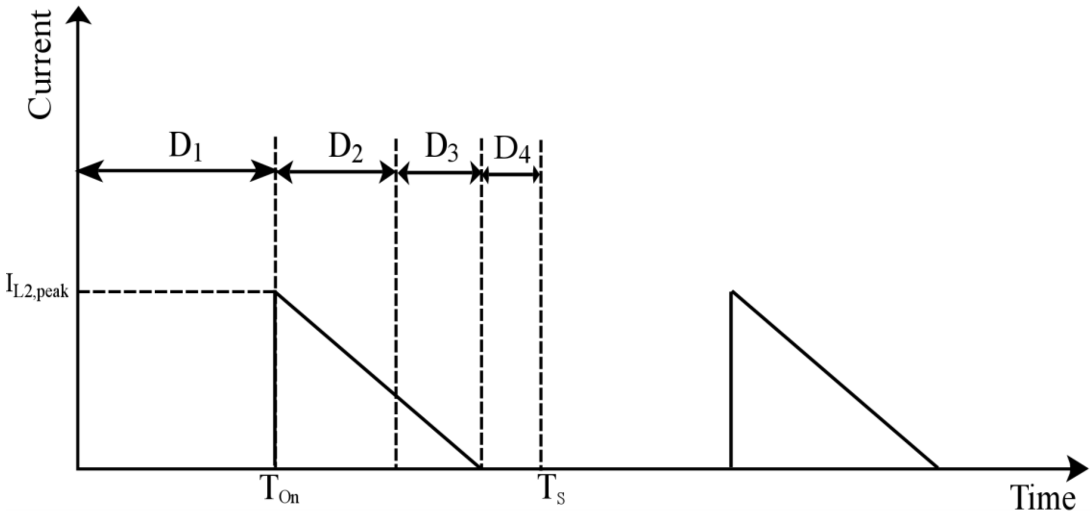

Figure 2.11: Current wave form of the Diode D4

$$\left\langle I_{D_4,rms} \right\rangle_{T_S} = I_{D_4,peak} \sqrt{\frac{D_2 + D_3}{3}} \tag{2.19}$$

Putting the values of D_2 and D_3 from equations (2.8),(2.10)in the above equation, we will get

$$\Rightarrow \left\langle I_{D_4,rms} \right\rangle_{T_S} = \frac{I_{D_4,peak}}{\sqrt{3}} \sqrt{D_1 \frac{\left|V_S(\theta)\right|}{V_{C_1}} + D_1 \left[\frac{V_{C_1} - V_O}{V_O} - \frac{\left|V_S(\theta)\right|}{V_{C_1}} \right]}$$

$$\Rightarrow \left\langle I_{D_4,rms} \right\rangle_{T_S} = \frac{\left(V_{C_1} - V_O\right)}{f_S L_2} \sqrt{\frac{\left(D_1\right)^3}{3}} \sqrt{\frac{V_{C_1} - V_O}{V_O}} \qquad (2.20)$$

Where

$$I_{D_4,peak} = \frac{\left(V_{C_1} - V_O\right)}{f_S L_2} D_1$$

The formula for the r.m.s current over the half-line period $\left(\frac{T_L}{2}\right)$ can be found out by integrating over the half-line period

$$\left\langle I_{D_4,rms} \right\rangle_{\frac{T_L}{2}} = \frac{\left(V_{C_1} - V_O\right)}{f_S L_2} \sqrt{\frac{\left(D_1\right)^3}{3}} \sqrt{\frac{V_{C_1} - V_O}{V_O}} \qquad (2.21)$$

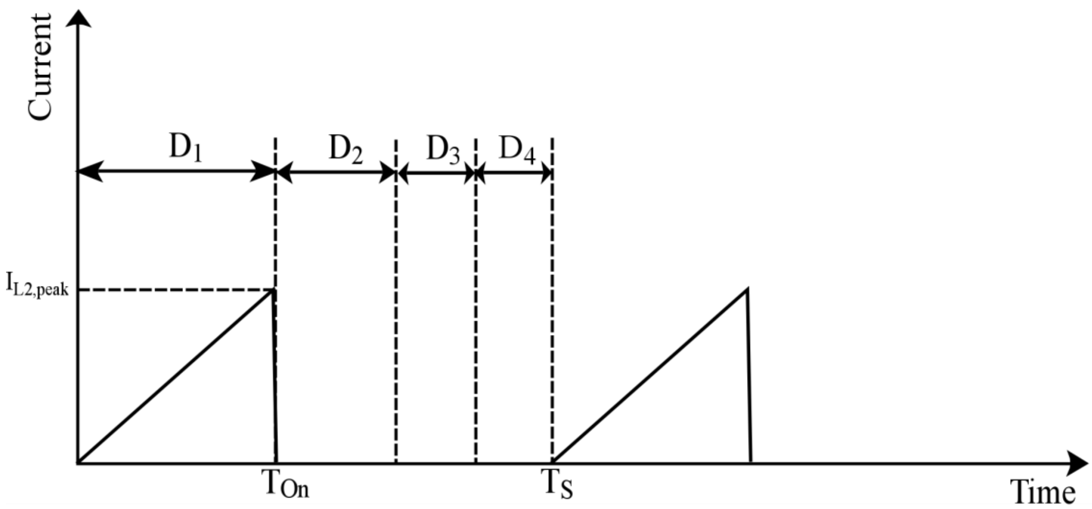

Figure 2.12: Current wave form of the Switch S2 and Diode D1

$$\left\langle I_{S_2,rms} \right\rangle_{T_S} = I_{S_2,peak}\sqrt{\frac{D_1}{3}} \tag{2.22}$$

From Figure (2.5), it is apparent that the current flowing through S_2 and D_1 are identical

$$\Rightarrow \left\langle I_{S_2,rms} \right\rangle_{T_S} = \left\langle I_{D_1,rms} \right\rangle_{T_S} = \frac{\left(V_{C_1} - V_O\right)}{f_S L_2}\sqrt{\frac{\left(D_1\right)^3}{3}} \tag{2.23}$$

Where

$$I_{S_2,peak} = I_{D_1,peak} = \frac{\left(V_{C_1} - V_O\right)}{f_S L_2} D_1$$

The formula for the r.m.s current over the half-line period $\left(\frac{T_L}{2}\right)$ can be found out by integrating over the half-line period

$$\left\langle I_{S_2,rms} \right\rangle_{\frac{T_L}{2}} = \left\langle I_{D_1,rms} \right\rangle_{\frac{T_L}{2}} = \frac{\left(V_{C_1} - V_O\right)}{f_S L_2}\sqrt{\frac{\left(D_1\right)^3}{3}} \tag{2.24}$$

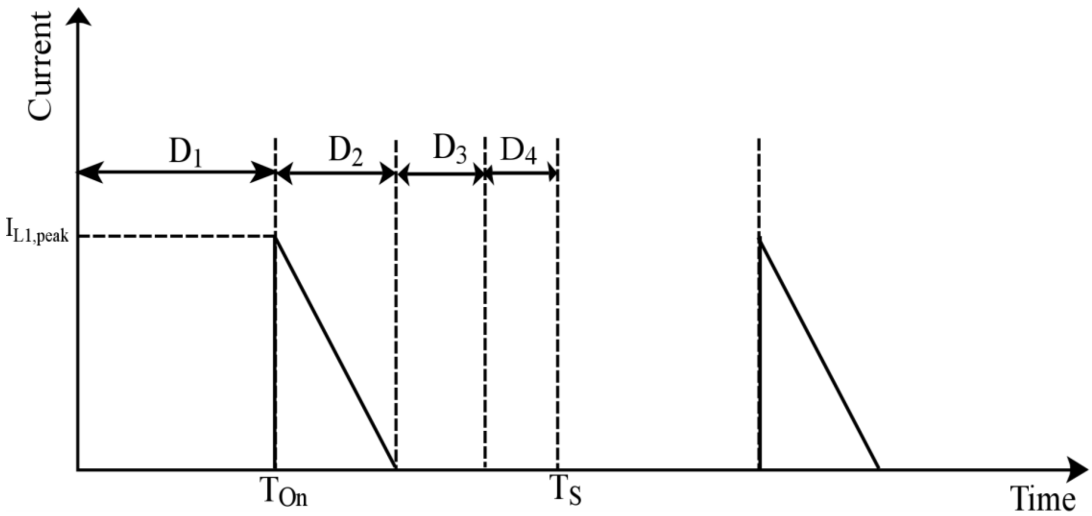

Figure 2.13: Current wave form of the Diodes D2 and D3

$$\left\langle I_{D_2,rms} \right\rangle_{T_S} = \left\langle I_{D_3,rms} \right\rangle_{T_S} = I_{L_1,peak}\sqrt{\frac{D_2}{3}} \tag{2.25}$$

Using the value of D_2 from Equation (2.8) ,we will get

$$\Rightarrow \left\langle I_{D_2,rms} \right\rangle_{T_S} = \left\langle I_{D_3,rms} \right\rangle_{T_S} = I_{L_1,peak} \sqrt{\frac{D_1}{3}} \sqrt{\frac{|V_S(\theta)|}{V_{C_1}}}$$

$$\Rightarrow \left\langle I_{D_2,rms} \right\rangle_{T_S} = \left\langle I_{D_3,rms} \right\rangle_{T_S} = \frac{|V_S(\theta)|}{f_S L_1} \sqrt{\frac{(D_1)^3}{3}} \sqrt{\frac{|V_S(\theta)|}{V_{C_1}}} \qquad (2.26)$$

Where

$$I_{D_2,peak} = I_{D_3,peak} = \frac{|V_S(\theta)|}{f_S L_1} D_1$$

The formula for the r.m.s current over the half-line period $\left(\frac{T_L}{2}\right)$ can be found out by integrating over the half-line period

$$\left\langle I_{D_2,rms} \right\rangle_{\frac{T_L}{2}} = \left\langle I_{D_3,rms} \right\rangle_{\frac{T_L}{2}} = \frac{1}{\pi f_S L_1} \sqrt{\frac{(D_1)^3}{3}} \int_0^{\pi} |V_S(\theta)| \sqrt{\frac{|V_S(\theta)|}{V_{C_1}}} d\theta \qquad (2.27)$$

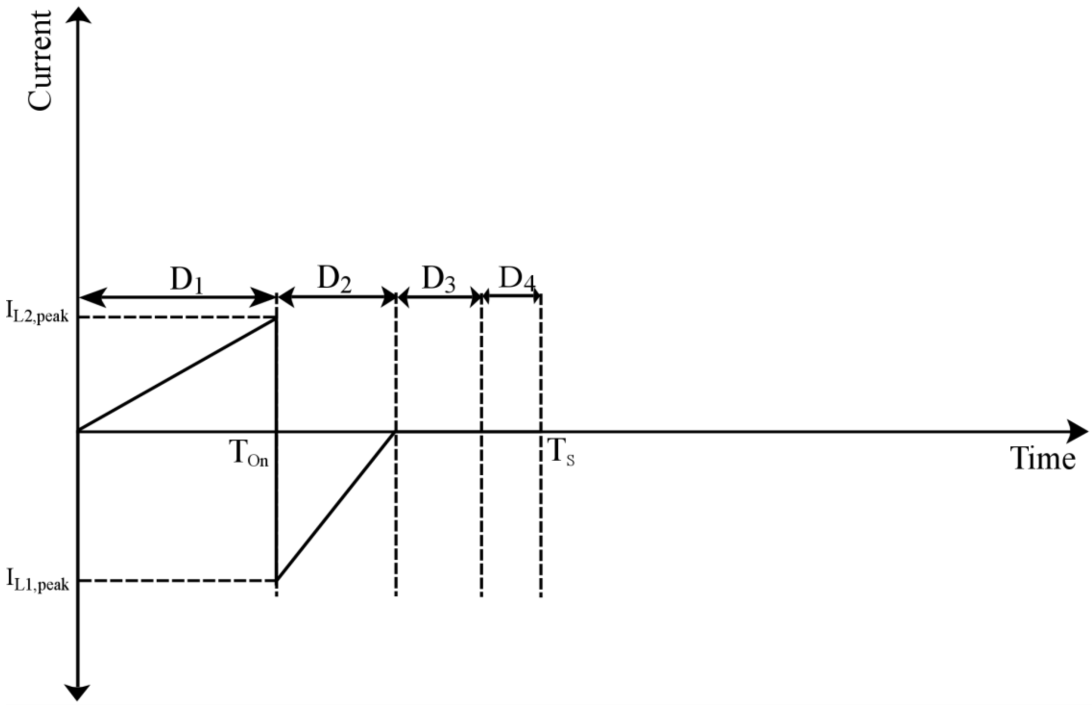

Figure 2.14: Current wave form flowing through C_1

From Figure 2.14

$$\left\langle I_{C_1,avg} \right\rangle_{T_S} = \frac{1}{2}\left(I_{L_2,peak} D_2 - I_{L_1,peak} D_1 \right)$$

$$\Rightarrow \left\langle I_{C_1,avg} \right\rangle_{T_S} = \frac{D_1^2}{2 f_S}\left[\frac{\left(V_{C_1} - V_O\right)}{L_2} - \frac{\left|V_S(\theta)\right|^2}{V_{C_1} L_1} \right] \tag{2.28}$$

The formula for the r.m.s current over the half-line period $\left(\frac{T_L}{2}\right)$ can be found out by integrating over the half-line period

$$\left\langle I_{C_1,avg} \right\rangle_{\frac{T_L}{2}} = \frac{1}{\pi}\int_0^{\pi} \frac{D_1^2}{2 f_S}\left[\frac{\left(V_{C_1} - V_O\right)}{L_2} - \frac{\left|V_S(\theta)\right|^2}{V_{C_1} L_1} \right] d\theta \tag{2.29}$$

Assuming that the current through the capacitor reach a steady state over a half-line, we will equate the above equation to zero

$$\Rightarrow V_{C_1} - V_O = \frac{L_2 V_m^2}{2 L_1 V_{C_1}} \tag{2.30}$$

Calculation of Approximate value of D_1

Method 1:

Calculation of D_1 is done as described below[17, 18]. Figure2.8. resembles the output current over one switching cycle. The average value of the output current over the switching cycle

$$\left\langle I_{O,avg} \right\rangle_{T_S} = \frac{1}{2} \times \left(D_1 + D_2 + D_3 \right) \times I_{L_2,peak} \tag{2.31}$$

Using the Equations(2.15) and (2.17)

$$\left\langle I_{O,avg} \right\rangle_{T_S} = \frac{D_1^2}{2 f_S} \left[\frac{V_{C_1} - V_O}{L_2} \right] \left[\frac{V_{C_1}}{V_O} \right] \tag{2.32}$$

Solving the Equation (2.38)

$$D_1 = \sqrt{\frac{2 V_O I_O f_S L_2}{V_{C_1} \left(V_{C_1} - V_O \right)}} \tag{2.33}$$

Solving the Equation(2.30) and Equation(2.33) and neglecting the ripple in V_{C_1}, we will get D_1 as .15

Method 2:

From Equation(2.7), we can get an approximate value D_1 by using all the operating conditions

i.e.

$V_m = 155.54v$

$f_S = 48kHz$

$R_{load} = 80\Omega$

$L_1 = 140\mu\text{H}$

$V_O = 40v$

With above values, we will get D_1 approximately equal to .15

Calculation of the buck-boost inductor

The gain of the system when both the stages are operating in critical conduction mode

$$\frac{V_O}{V_S} = \frac{D_1^2}{\left(1 - D_1\right)} \qquad (2.34)$$

Using the operating conditions (i.e. V_O and V_S), D_{1crit} can be calculated. Using the Equation (2.5) and D_{1crit}, the buck-boost critical inductance value $L_{1,crit}$ can be calculated. To make the input buck-boost converter operate in DCM, we need to take inductance value lesser than that.

Under the rated condition (i.e. $V_O = 40v$ and $V_S = 155.54v$), solving equations (2.5) and (2.34), the value of $L_{1,crit}$ can be calculated as 978.64µH. If we use any inductance $L_1 < L_{1,crit}$ the input buck-boost stage will operate in DCM. For the present application, L_1 is selected as 140µH.

Calculation of the buck inductor

The output buck converter is being operated in discontinuous conduction mode. For finding the required L_2, we have to analyze by taking the output buck converter in critical conduction mode.

$$\Delta I = \frac{V_S D_1 \left(1 - D_1\right)}{f_S L_2} \qquad (2.35)$$

Equation (2.35) is an expression for the ripple content in the inductor current valid for both critical and continuous conduction mode .For critical conduction mode,

$$\Delta I = 2I_O \qquad (2.36)$$

Using Equation (2.35) and $D_{1,crit}$ from Equation (2.36), $L_{2,crit}$ can be calculated. We need to select $L_2 <$ $L_{2,crit}$ for the buck converter to operate in DCM.

Under the rated condition (i.e. $V_O = 40v$,$V_S = 155.54v$ and $R_{load} = 80\Omega$), solving equations (2.35) and (2.36), the value of $L_{2,crit}$ can be calculated as 770.2µH. If we use any inductance $L_2 < L_{2,crit}$, the input buck-boost stage will operate in DCM. For the present application, is selected as 90µH.

Calculation of the storage capacitor

Calculation of the storage capacitor is done using the below written formula [15]

$$\Delta V_{C_1} = \frac{D_1^2 V_S^2}{8\pi V_{C_1} L_1 C_1 f_s f_l} \tag{2.37}$$

Calculation of capacitor is done after calculations of V_{C_1} from Equation (2.36) and D_1 from Equation (2.33). With 5% ripple (i.e. $\Delta V_{C_1} = 0.05 \times V_{C_1}$),from Equation (2.37) C_1 can be calculated as 106.6µF. For the present application C_1 is taken as 100µF

Table 2.1: Theoretical Voltage ratings of the semiconductor switches

Switches	PIV across the switch
Mosfet S_1	$V_m + V_{C_1}$
Mosfet S_2	$V_m + V_{C_1}$
Diode D_1	V_m
Diode D_2	V_m
Diode D_3	V_{C_1}
Diode D_4	V_{C_1}

Table 2.2: Theoretical Voltage ratings of the Inductors

Inductor	Voltage
L_1	V_m
L_2	$V_{C_1} - V_O$

Table 2.1 and Table 2.2 contain the theoretical voltage ratings of semiconductor switches and the inductors. The values obtained from mathematical formulae are compared with the simulation results in the last section which will help us choose device of proper voltage ratings.

2.3.2 Voltage Controller ic

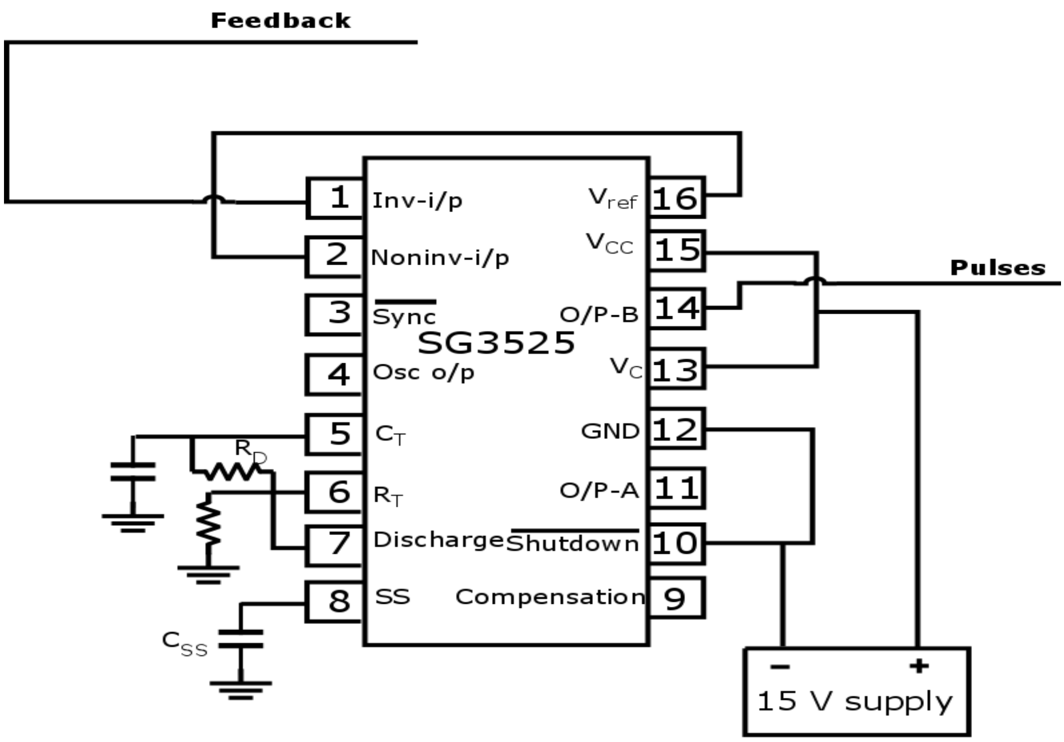

Figure 2.15: Pin diagram of the SG3525 voltage controller IC

A universal voltage controller ic SG3525 is used for controlling the output voltage. The Voltage controller ic and the block diagram are shown in Figures 2.15 and 2.16 respectively [27, 28]. Pins 1 (Inverting Input) and 2 (Non Inverting Input) are the inputs to the on-board error amplifier. It is like a comparator which increases or decreases the duty cycle depending on the feedback and the voltage level on the non-inverting input Pin-2 respectively.

Duty cycle increases when the feedback voltage is greater than the voltage on the Non-Inverting Input.

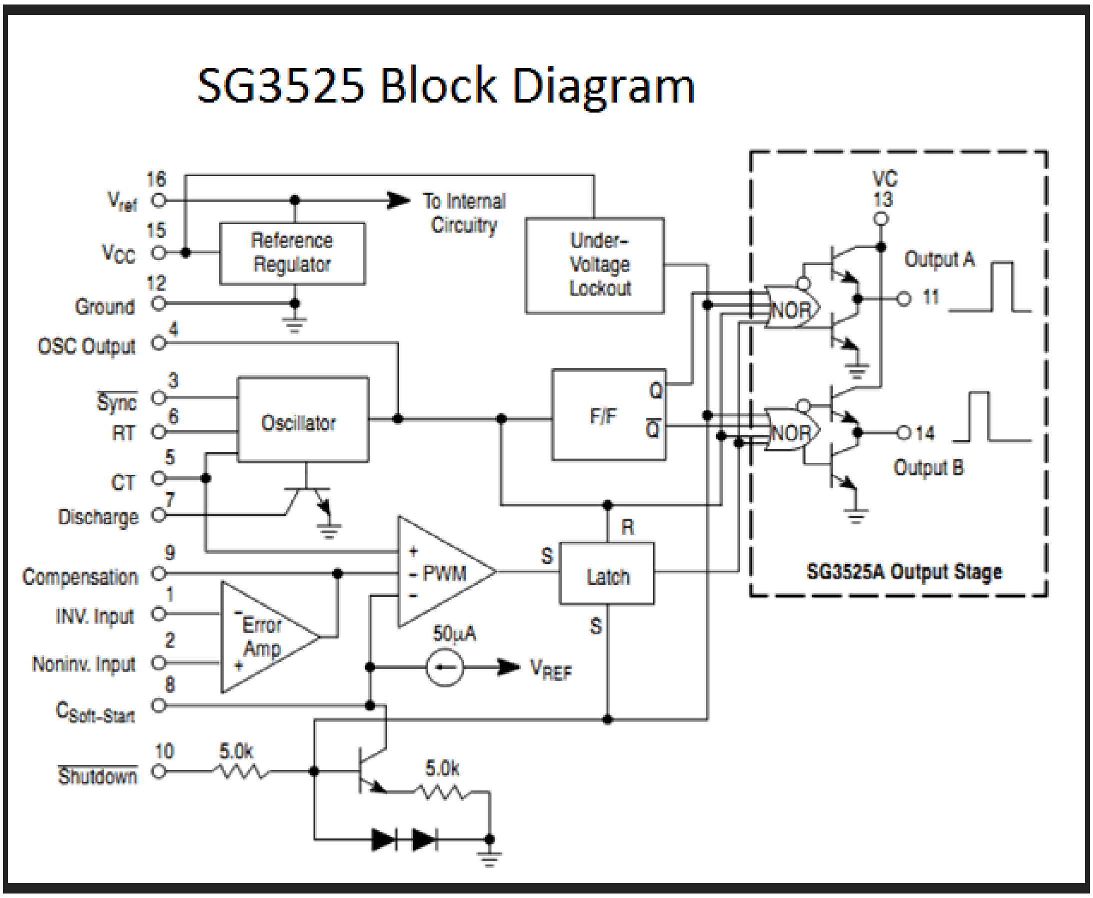

Figure 2.16: Block diagram of SG3525 voltage controller IC

Duty cycle decreases when the voltage on the Non-Inverting Input is greater than the feedback voltage.

The PWM frequency is decided by C_T and R_T which are connected between Pins 5,6 and ground respectively. The resistance between pins 5 and 7 $\left(R_D\right)$ determines the deadtime (and also slightly affects the frequency).

$$f_S = \frac{1}{C_T\left(.7R_T + R_D\right)} \tag{2.38}$$

Equation (2.38) denotes the switching frequency.

Chapter 3

Simulation Results

Table 3.1: Circuit components used for simulation

Components	Value
L_1	$140\mu H$
L_2	$90\mu H$
C_1	$100\mu F$
C_o	$200\mu F$

Table 3.1 contains the circuit components used for the simulation studies. The value of the components are calculated using the formulae derived in the previous section Generally EMI filters are used at the front end of PFC rectifiers for reduction of radiated as well as conducted EMI. The primary objective here is to design a prototype of a PFC converter instead of designing EMI filter. Hence, filter components are chosen based on the availability in the laboratory so that we can use the same for hardware implementation.

Table 3.2: Filter components used for simulation

Components	Value
L_f	$1m\text{H}$
C_f	$1\mu F$

Table 3.3: Circuit Specifications

Specification	Value
Supply Voltage (V_S)	$110V_{rms}$,50Hz
Switching Frequency (f_s)	48kHz
Output Power (P_O)	20 W
Load Voltage (V_O)	40 V
Equivalent Load Resistance (R_{load})	80Ω

The results are shown below

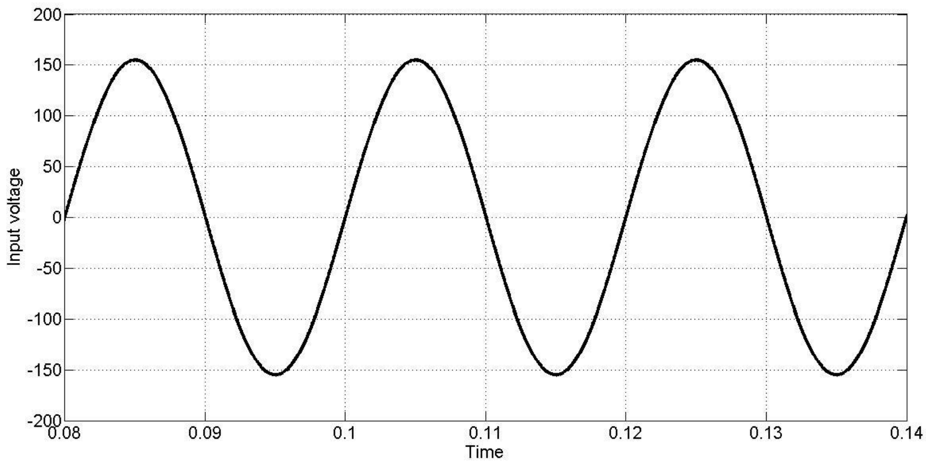

Figure 3.1(a): Simulation results of the supply voltage

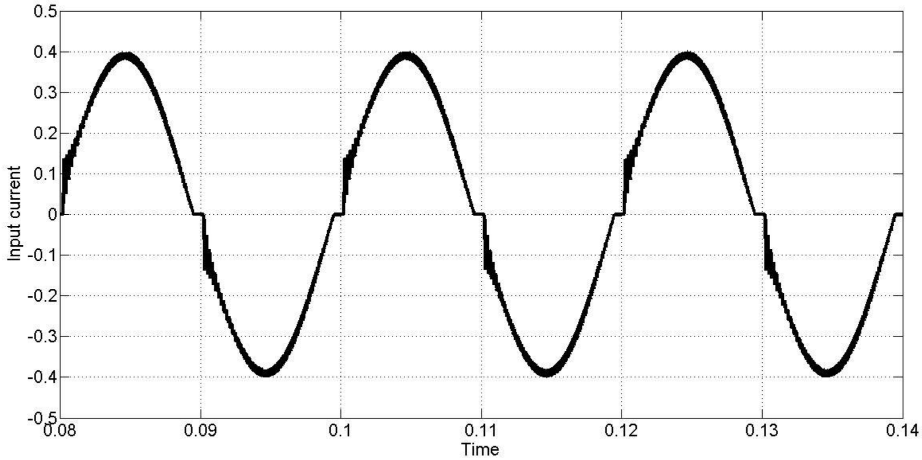

Figure 3.1(b): Simulation results of the supply current

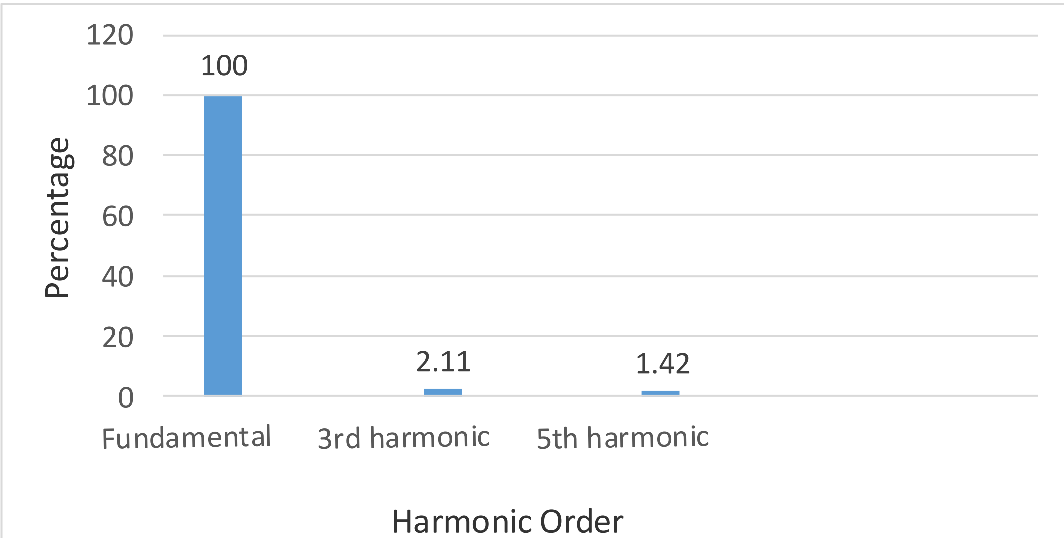

Figure 3.2: Harmonic content of the supply current relative to the fundamental

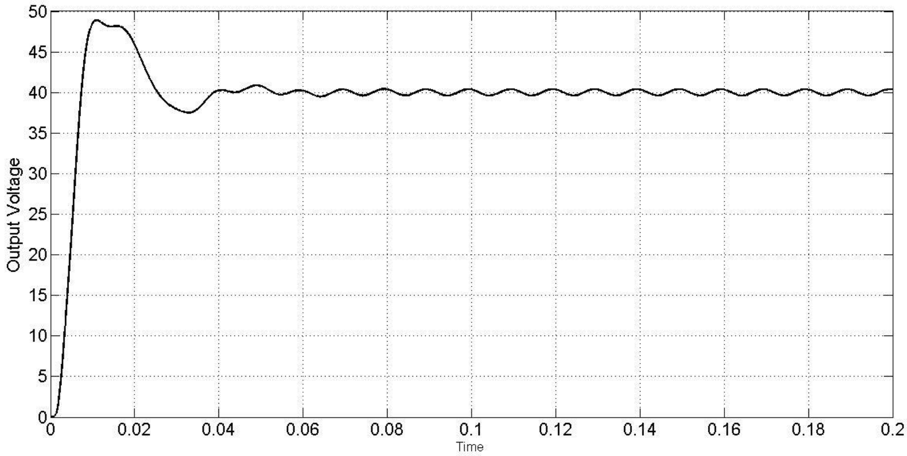

Figure 3.3: Simulation result of the Load voltage

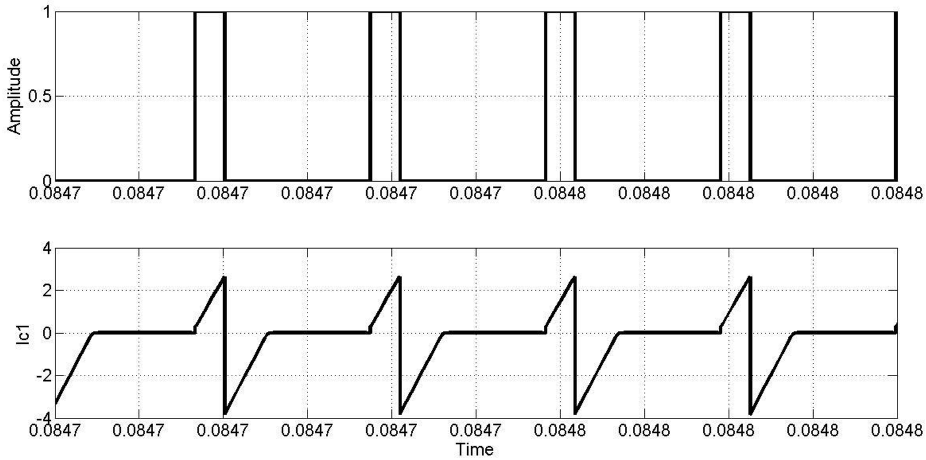

Figure 3.4: Simulation results of the gate pulse and storage capacitor current

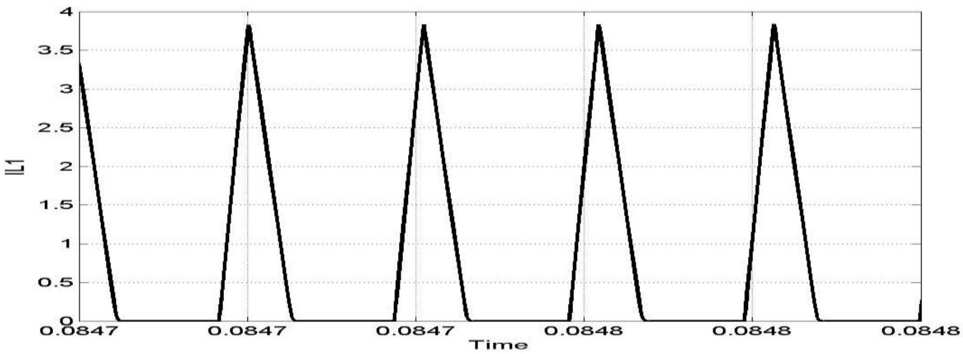

Figure 3.5: Simulation results of the inductor L_1 current

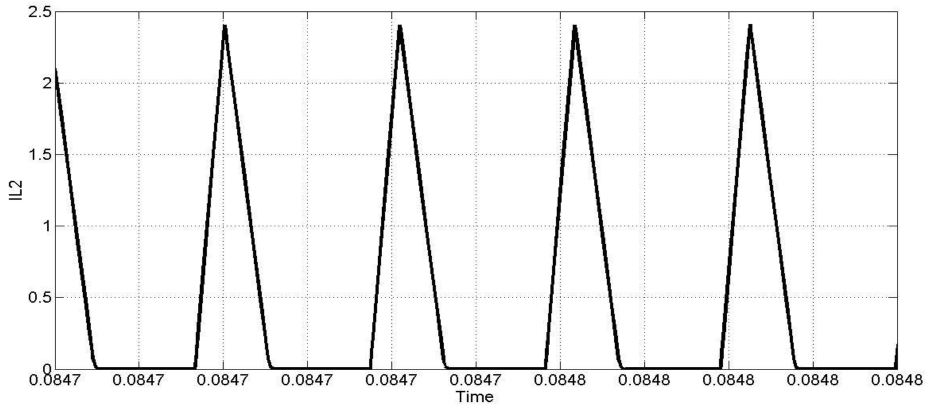

Figure 3.6: Simulation results of the inductor L_2 current

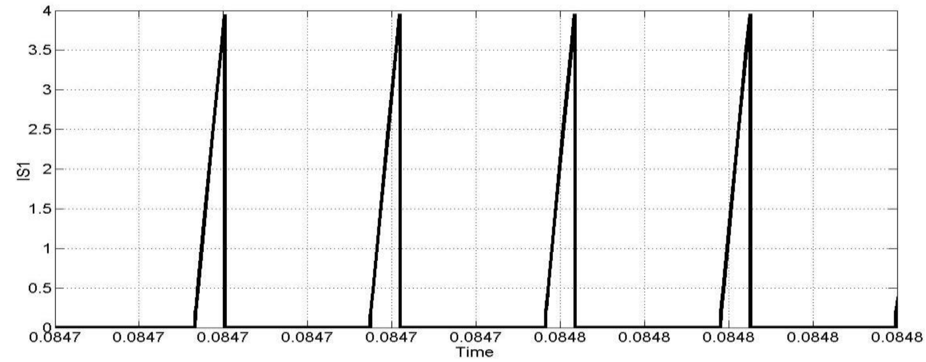

Figure 3.7: Simulation results of the Mosfet S_1 current

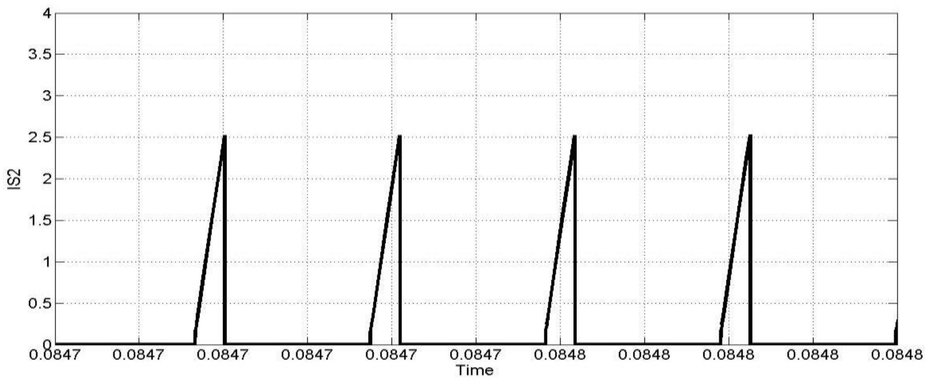

Figure 3.8: Simulation results of the Mosfet S_2 current

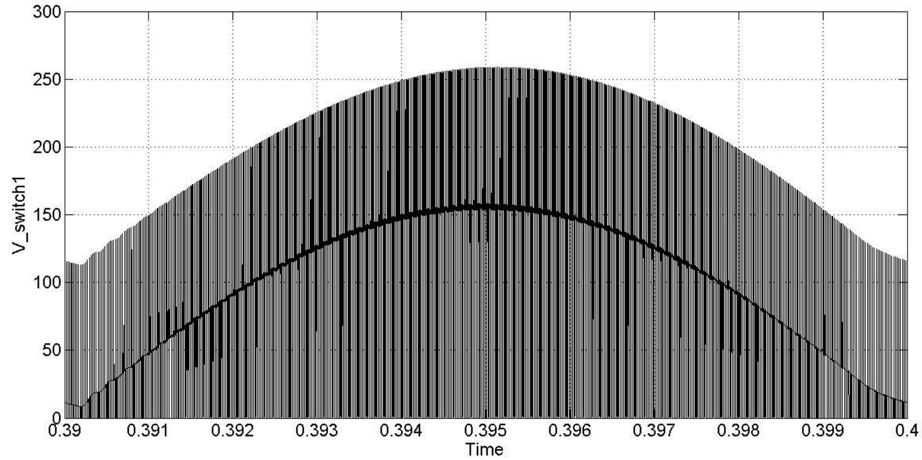

Figure 3.9: Simulation results of the voltage across the switch S_1

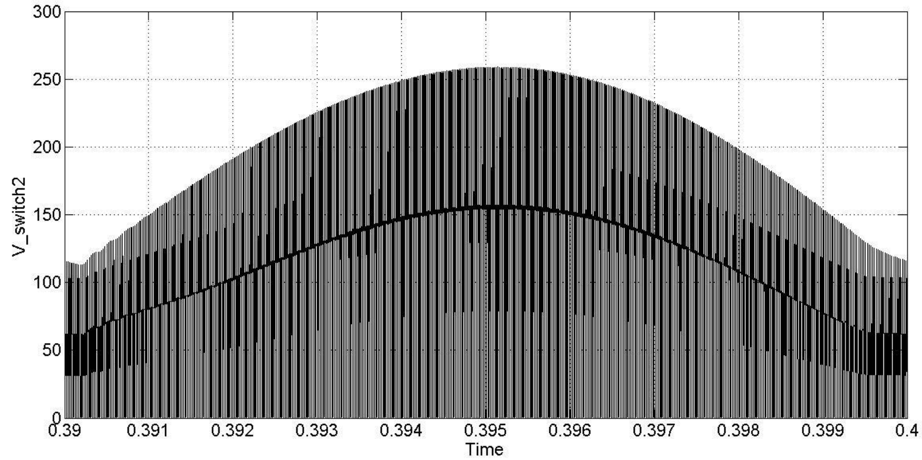

Figure 3.10: Simulation results of the voltage across the switch S_2

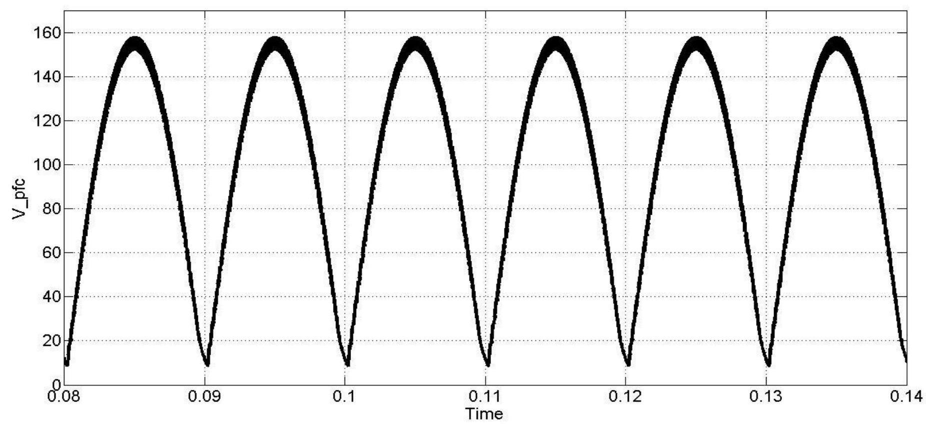

Figure 3.11: Simulation results of the input voltage to the PFC rectifier

Chapter 4

Hardware implementation and Results

4.1 Hardware Implementation

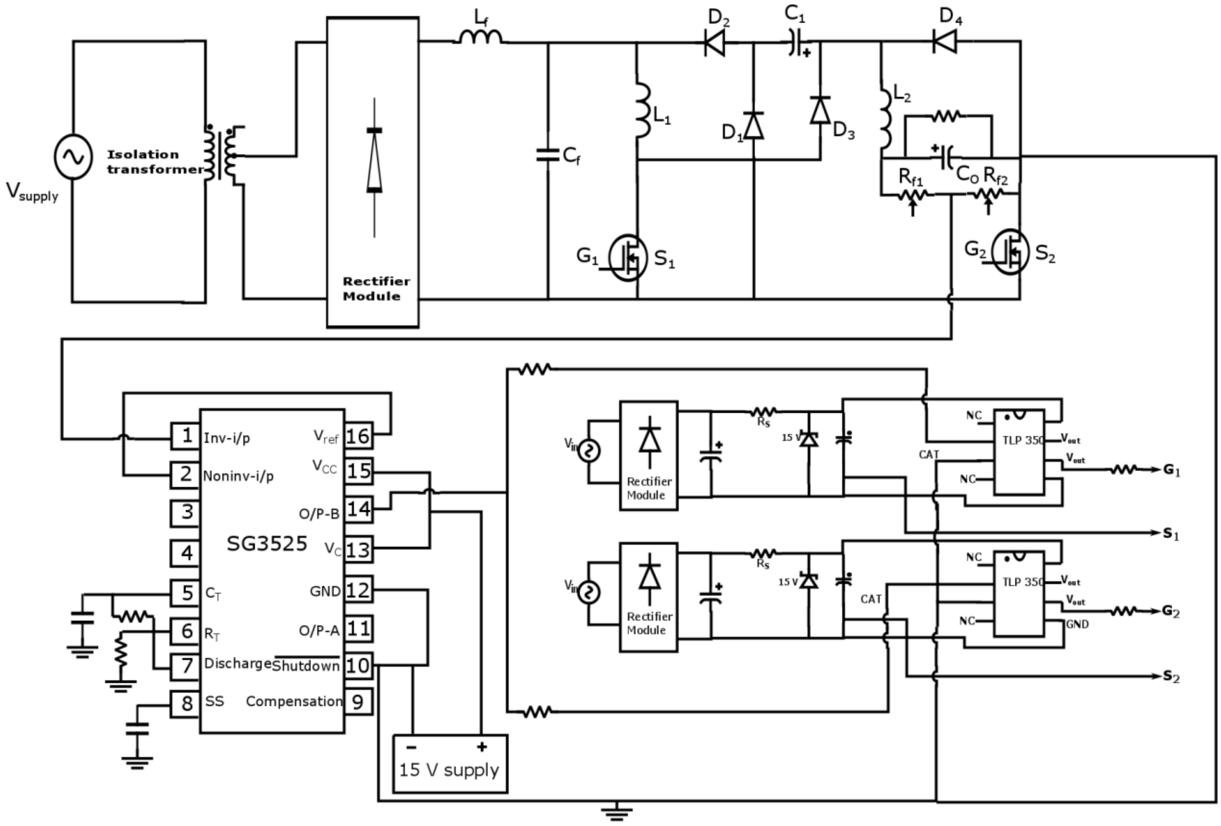

Figure 4.1: Complete circuit diagram of proposed PFC converter circuit

Proposed PFC circuit is designed for input 110Vrms and output 40 volt (DC). A proto type of this PFC circuit is developed in the laboratory. The schematic of the circuit is given in Figure 4.1.

Table 4.1: Component Rating Comparison

Components	Current Rating(maximum)(A)		Voltage Rating(V)	
	From Formulae	From Simulation	From Formulae	From Simulation
Mosfet S_1	3.84	3.95	265.54	258.3
Mosfet S_2	2.69	2.65	265.54	258.3
Diode D_1	2.69	2.65	155.54	153.8
Diode D_2	3.84	3.85	155.54	158.3
Diode D_3	3.84	3.85	110	116
Diode D_4	2.69	2.52	110	117
Inductor L_1	3.84	3.85	155.54	117
Inductor L_2	2.69	2.52	70	78

Table 4.1 contains voltage as well as current ratings of different components. These ratings calculated from the formulae derived in the previous section are compared with the ratings observed from the simulation. It can be seen that both the ratings are almost equal. Hence, the components are selected with similar ratings for hardware implementation.

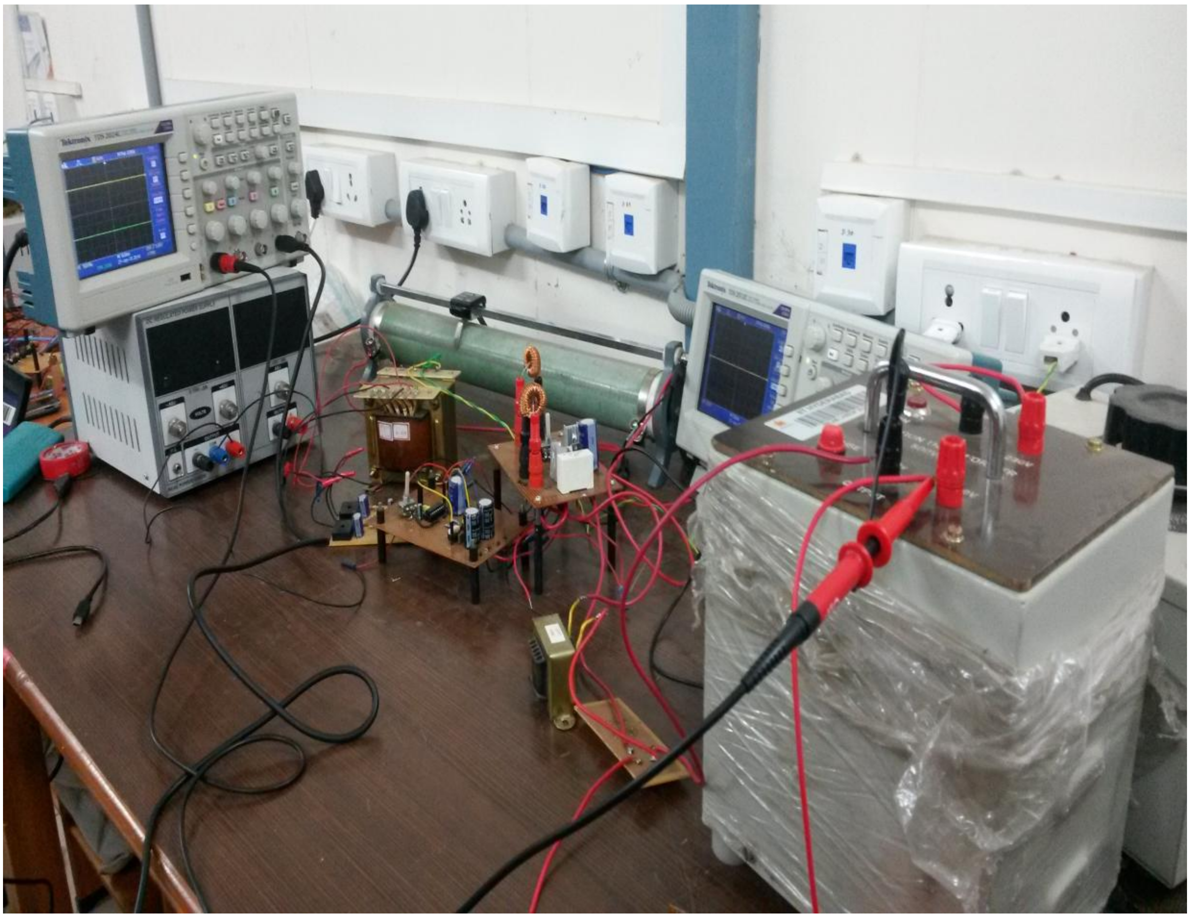

Figure 4.2: Experimental Set up

4.2 Experimental result

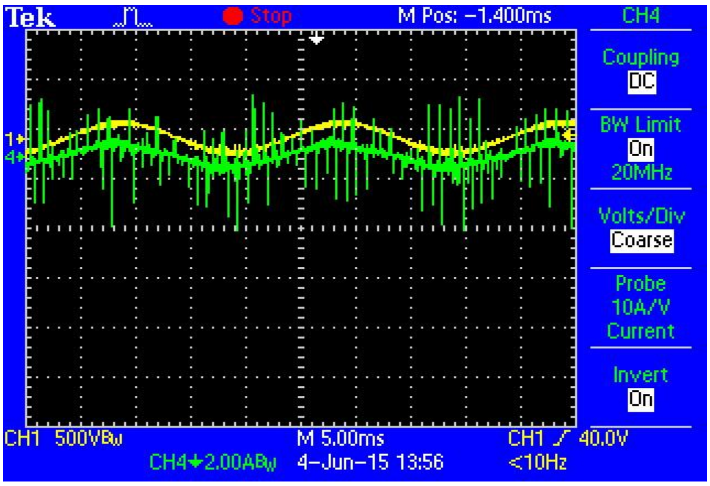

Figure 4.3(a): Input voltage Vs Input current

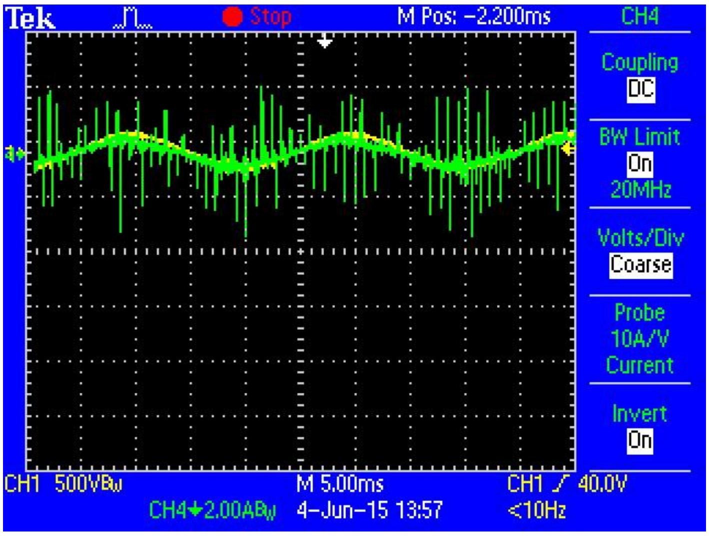

Figure 4.3(b): Input voltage Vs Input current (superimposed)

In the Figure4.3(a) and Figure4.3(b), the yellow one is the supply voltage and the green one is the supply current respectively. The input voltage and the input current are almost in same phase resulting in a pf close to unity. In the above figures X-axis is the time axis and Y-axis is the input voltage axis/current axis. It can be seen that the current waveform is satisfying all the angle conditions between the supply voltage and supply current as set by EN61000-3-2 class C regulations.

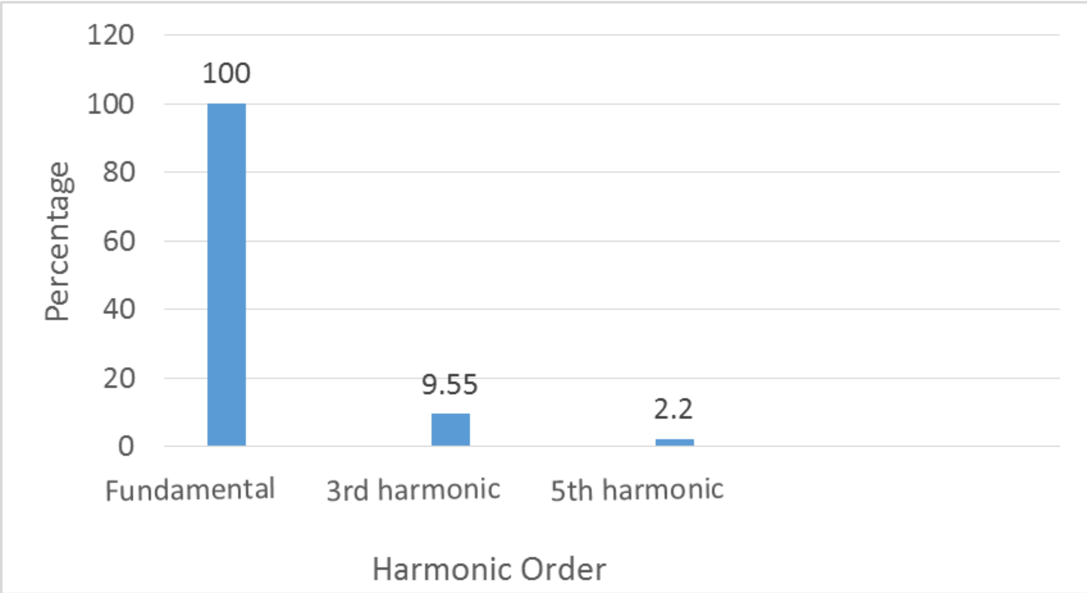

Figure 4.4: Harmonic content of the supply current relative to the fundamental

Figure 4.4 shows the relative harmonic (3rd ,5th)with respect to the fundamental. It can be seen that it satisfies all the harmonic conditions as set be EN61000-3-2 class C regulations

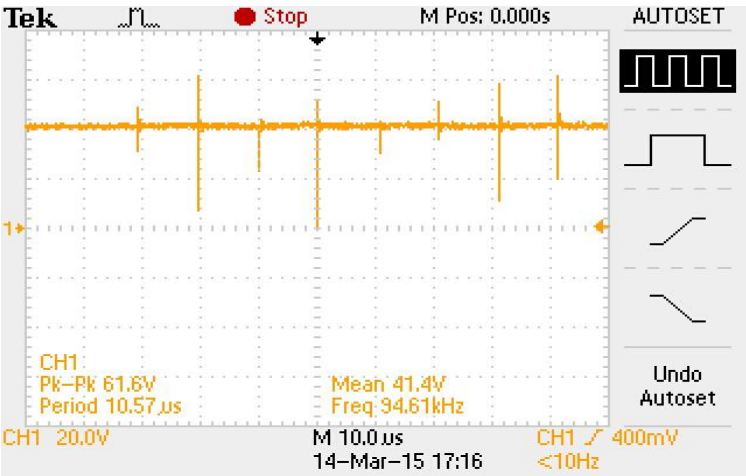

Figure 4.5: Output voltage for 20W load

Figure 4.5 shows the load voltage. The desired load voltage is 40volt. The load voltage is almost constant with a very less amount of ripple content (<0.01%). The constant load voltage is a primary requirement for driving HB-LEDs which is successfully achieved by closed loop controller. In the above figures X-axis is the time axis and Y-axis is the output voltage axis.

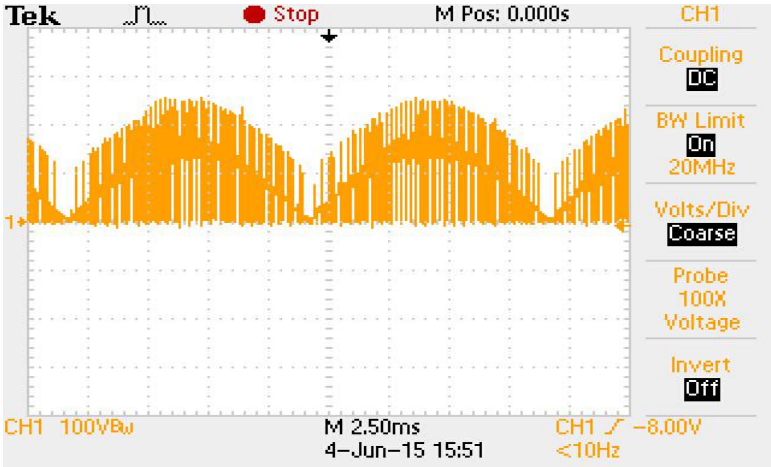

Figure 4.6: Voltage profile across switch S_1

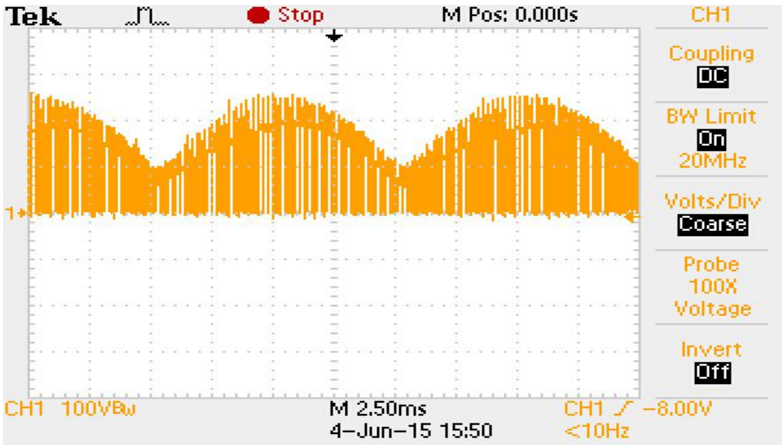

Figure 4.7: Voltage profile across switch S_2

The Figure 4.6 and 4.7 show the input voltage across the switch S_1 and switch S_2 respectively which are well in agreement with the simulation results we got in the previous section. In the above figures X-axis is the time axis and Y-axis is the voltage axis.

4.3 Transient study

Transient study is essential for analyzing the controller behavior in case of a sudden change in the load or line variation. The PFC converter operation must not be affected by undue oscillations resulting out of the transients. The function of the controller is to cause the output voltage to return to its steady state in minimum possible time without affecting the performance of the LEDs

- **Line Transient**

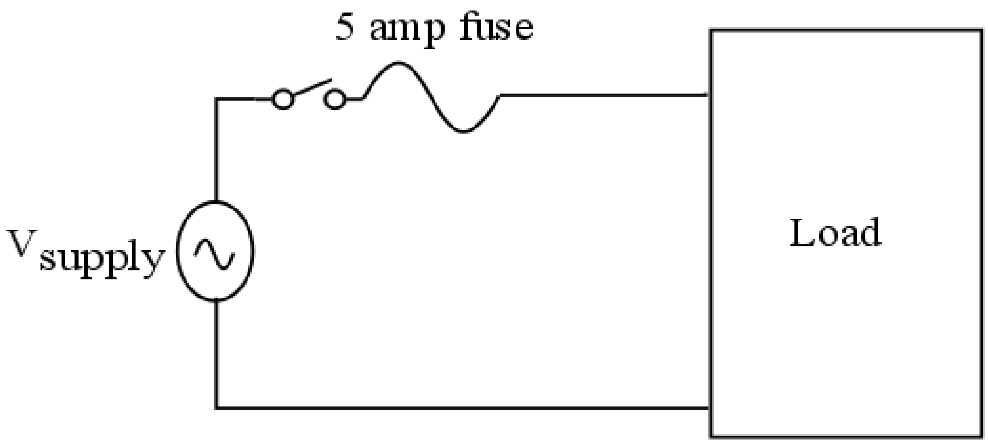

Figure 4.8: Set-up for studying line transient

Figure 4.8 shows the set-up used for analyzing the output voltage under the line transient. The supply voltage is suddenly applied at t=0. A 5 amp fuse is used for providing protection under any abnormal condition.

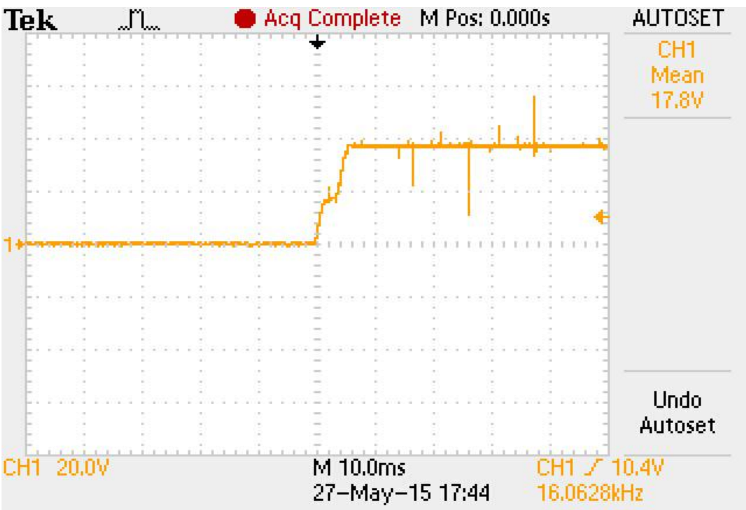

Figure 4.9: Output voltage under line transient

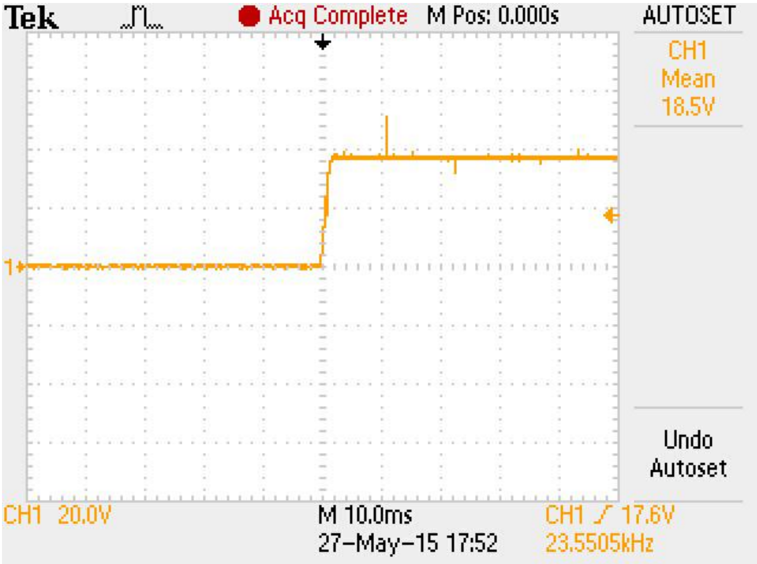

Figure 4.10: Output voltage under line transient

Figure4.9, 4.10 show the load voltage under line transient in two consecutive experiments. In both the experiments, it can be seen that the time taken by the output voltage to achieve the steady state output voltage is less than 6 millisec which is satisfactory.

- **Load transient**

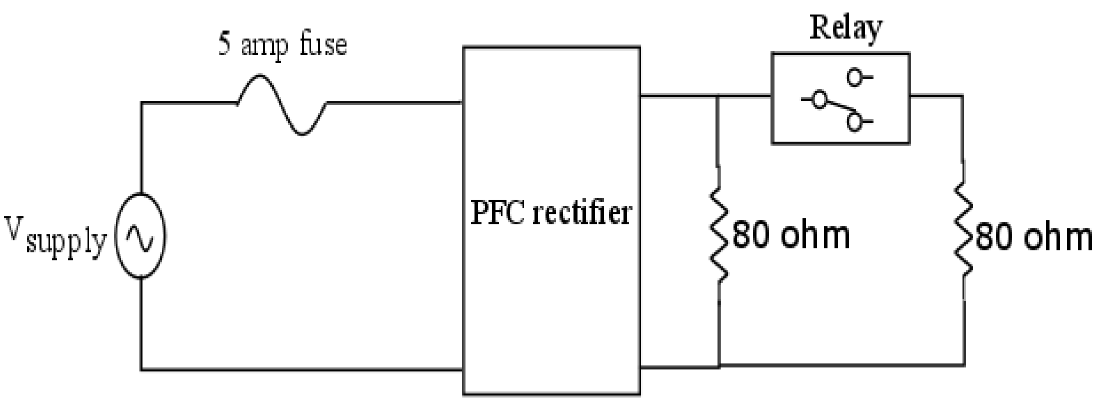

Figure4.11: Set-up for studying line transient

Figure4.11 shows the set-up used for creating a line transient like situation in laboratory environment. Two 80ohms are connected through a relay in the starting and are disconnected at a certain instant for creating load transient.

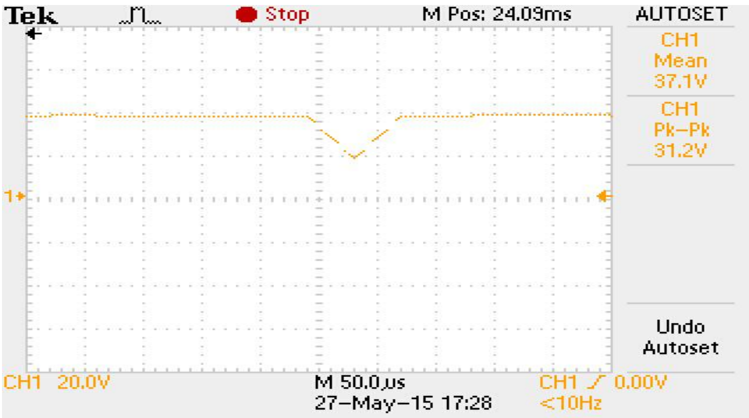

Figure 4.12: Output voltage under load transient

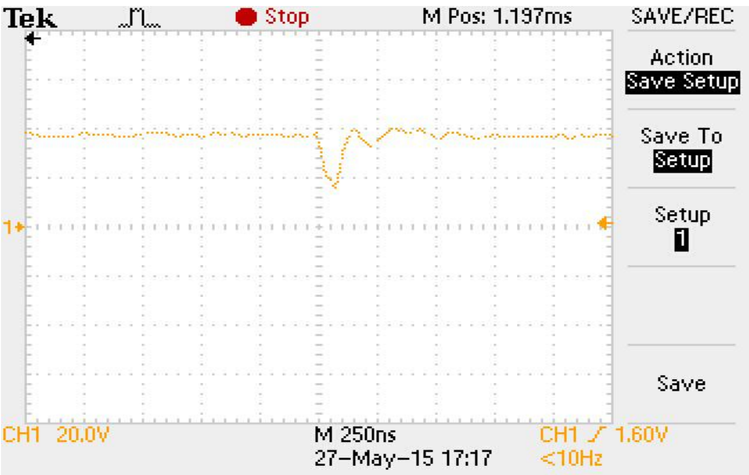

Figure 4.13: Output voltage under load transient

Conclusion

A Buckboost-Buck type PFC converter is proposed to drive HB-LEDs. The buck-boost converter is operated in DCM to improve the power-factor and lower the input current THD. The proposed converter is simulated in Matlab/Simulink. The input current and input voltage satisfy the general angle requirement as set by EN61000-3-2 class C regulation. The harmonic content of the input current is well below the requirement as set by EN61000-3-2 class C regulations. A prototype of the proposed non-inverting, integrated Buckboost-buck of 20 watt is designed and tested with a supply of 110Vrms. SG3525 IC is used as a voltage controller for controlling the output voltage. The input angle requirement and supply current THD are well within the norms laid down by IEC 61000-3-2 class C regulation. The DC voltage output is found to be almost constant which ensures that the current flowing through the LED lamp would remain constant.

References

[1.] I. L. Azevedo, M. G. Morgan, and F. Morgan, “The transition to solid-State lighting,” in Proc. IEEE, Mar. 2009,vol. 97, no. 3, pp. 481-510.

[2.] E. F. Schubert, Light-Emitting Diodes, 2nd ed. Cambridge, U.K.:Cambridge Univ. Press, 2006.

[3.] J. J. Sammarco. M. A. Reyes, J. R. Bartels, and Sean Gallagher, LED, Miner Cap Lamps," IEEE Transactions on Industry Applications, vol. 45 no. 6, pp. 1923-1929,November/December 2009.

[4.] M. S. Shur and R. Zukauskas, “Solid-state lighting: Toward superior illumination,” in Proc. IEEE, Oct. 2005, vol. 93, no. 10, pp. 1691–1703.

[5.] Garcia, O.; Cobos, J.A; Prieto, R.; Alou, P.; Uceda, J., "Single phase power factor correction: a survey," Power Electronics, IEEE Transactio n , vol.18, no.3, pp.749,755, May 2003.

[6.] Chuang, Ying-Chun, et al. "Single-stage power-factor-correction circuit with flyback converter to drive LEDs for lighting applications." Industry Applications Society Annual Meeting (IAS), 2010 IEEE. IEEE, 2010.

[7.] Zhu, G.; Wei, H.; Iannello, C.; Batarseh, I, "A study of power factor and harmonics in switched-mode power supplies," Southeastcon '99 Proceedi ngs. IEEE,vol., no., pp.278, 283, 1999.

[8.] Wei, H.; Batarseh, I, "Comparison of basic converter topologies for powe r factor correction," Southeastcon '98. Proceedings. IEEE , vol., no.,pp 348, 353, 24-26 Apr 1998.

[9.] Limits for Harmonic Current Emissions, International Electro technical Commission Standard, IEC-61000-3-2, 2004.

[10.] Fundamentals of Power Electronics by R.W.Erickson, D.Maksimovic, Springer Science &Business Media, Technology &Engineering, 2nd Edition.

[11.] Chakraborty, Arindam, Alireza Khaligh, and Ali Emadi. "Combination of buck and boost modes to minimize transients in the output of a positi ve buck-boost converter." In, IEEE Industrial Electronics IECON 2006-32nd Annual Conference on, pp. 2372-2377. IEEE, 2006.

[12.] Ismail, Esam H., Ahmad J. Sabzali, and Mustafa A. Al-Saffar. "Buck–boost-type unity power factor rectifier with extended voltage conversion ratio." Industrial Electronics, IEEE Transactions on 55.3 (2008): 1123-1132

[13.] Al-Saffar, M.A; Ismail, E.H.; Sabzali, AJ., "Integrated Buck–Boost–Buck PFC Rectifier for Universal Input Applications," Power Electronics, IEEE

[14.] Alonso, J.M.; Viña, J.; Vaquero, D.G.; Martinez, G.; Osorio, R., "Analysis and Design of the Integrated Double Buck–Boost Converter as a High-Power-Factor Driver for Power-LED Lamps," Industrial Electronics, IEEE Transactions on , vol.59, no.4, pp.1689,1697, April 2012.

[15.] Alonso, J. Marcos, et al. "A long-life high-power-factor HPS-lamp LED retrofit converter based on the integrated buck-boost buck topology topology." IECON 2011-37th Annual Conference on IEEE Industrial Electronics Society. IEEE, 2011.

[16.] Ki, Shu-Kong, and DD-C. Lu. "A high step-down transformerless single-stage single-switch AC/DC converter." Power Electronics, IEEE Transactions on 28.1 (2013): 36-45..

[17.] Ki, Shu-Kong, and DD-C. Lu. "Implementation of an efficient transformerless single-stage single-switch AC/DC converter." Industrial Electronics, IEEE Transactions on 57.12 (2010): 4095-4105.

[18.] Ki, Shu-Kong, and Dylan Dah-Chuan Lu. "Transformerless single-stage

AC/DC converter with direct power transfer." Power Engineering Conference, 2008. AUPEC'08. Australasian Universities. IEEE, 2008

[19.] Liang, T-J., L-S. Yang, and J-F. Chen. "Analysis and design of a single-phase AC/DC step-down converter for universal input voltage." IET Electric Power Applications 1.5 (2007): 778-784.

[20.] Cheng, Hung-Liang, et al. "A high-power-factor LED driver with zero-voltage switching-on characteristics." Power Electronics and Drive Systems (PEDS), 2013 IEEE 10th International Conference on. IEEE, 2013.

[21.] Lamar, Diego G., et al. "Tapped-inductor buck HB-LED AC–DC driver operating in boundary conduction mode for replacing incandescent bulb lamps." Power Electronics, IEEE Transactions on 27.10 (2012): 4329-4337.

[22.] http://www.homedepot.com/p/Philips-60-Watt-Incandescent-A19-Household- Light-Bulb-4-Pack-374843/100080337#.UBGxerR8Dg8

[23.] http://www.homedepot.com/p/Philips-EcoVantage-60-Watt-Halogen-A19-Soft- White-Dimmable-Light-Bulb-4-Pack-426031/203637006.

[24.] http://www.homedepot.com/s/100687000.

[25.] http://www.homedepot.com/p/Cree-60W-Equivalent-Soft-White-2700K-Dimmable-LED-Light-Bulb-BA19-08027OMF-12DE26- 2U100/204592770?N=5yc1vZbm79

[26.] http://www.grainger.com/product/LEDNOVATION-LED-Lamp-WP131798/_/N-9h9Z1z061o7

[27.] http://www.onsemi.com/pub_link/Collateral/SG3525A-D.PDF

[28.] http://tahmidmc.blogspot.in/2013/01/using-sg3525-pwm-controller-explanation.html